GÖTEBORGS UNIVERSITET
Institutionen för geovetenskaper
Avdelningen för oceanografi
Geovetarcentrum

SUSPENDED SEDIMENT TRANSPORT AND EXCHANGE IN PORT REITZ CREEK WITH SPECIAL FOCUS ON THE MANGROVE FRINGED MWACHE WETLAND, KENYA

Johnson U. Kitheka

ISSN 1400-3821

B231
Projektarbete
Göteborg 2000

Postadress
Box 460
Geovetarcentrum
S-405 30 Göteborg

Besöksadress
Geovetarcentrum
Guldhedsgatan 5A

Telefon
031-773 28 70

Telfax
031-773 28 88

Earth Sciences Centre
Göteborg University
S-405 30 Göteborg
SWEDEN

ACKNOWLEDGEMENT

I gratefully acknowledge the support received from the International Foundation for Science (IFS) and Swedish Agency for International Development (Sida) through the SAREC Marine Science Program. I would like in particular to thank Prof. Lars Rydberg and Dr.Ulf Cederlof of the Department of Oceanography, University of Gothenburg in Sweden for their constructive advice and guidance throughout the course of this research. I would also like to thank Prof. Olof Linden of the University of Stockholm, the coordinator of the Marine Science Program, for his administrative role in the SAREC project. Mention must be made of Mr James Muhoro, the acting Director of the Kenya Marine and Fisheries Research Institute (KMFRI) and Mr Rennison Ruwa, Deputy-Director, for facilitating the continued co-operation between KMFRI and Sida. Their concerted support has been encouraging. I would also like to thank my colleagues at KMFRI for their support and encouragement.

The location map of the study area was drawn by Agneta Malm of the Gothenburg University, using an aerial photograph provided to the author by Prof. Richard S. Odingo of the Department of Geography, University of Nairobi, Kenya.

I am indebted to KMFRI technologists and technicians, messrs. Joseph Kamau, Joseph Kilonzo and M. Obiero who assisted in carrying out the fieldwork and laboratory assignments on sediment filtration and particle size analysis. I must not forget coxswains (messrs. Gaya, Omondi and Ayoyi) whose expertise and knowledge of the Port-Reitz mangrove creek helped us reach our sampling stations in time. I would also like to thank the divers, messrs. Ndirangu and Masudi of KMFRI who helped in mooring of the MicroTide pressure gauges and current meters at Miritini sediment monitoring station. I also convey my gratitude to drivers (messrs. Bonyi and Chiteri) for their patient and co-operation throughout the course of the study. I also express my gratitudes to Mzee Juma and Mwijuma, our two watchmen at Miritini for their assistance in guarding oceanographic instruments deployed at Miritini sediment monitoring station.

ABSTRACT

This study deals with the dynamics of water exchange and sediment flux in the 17 Km^2 mangrove–fringed Mwache mangrove wetland in Kenya. The study was implemented in the period between March 1998–March 1999. The creek experiences semi-diurnal tides with a spring tidal range of 3 m. It receives freshwater only in rainy seasons, mainly from Mwache and Bome rivers whose total catchment area is 1900 Km^2 and river discharge is less than 10 m^3/s in normal rainfall years. There is usually no river discharge in dry seasons.

The aim of the study was to determine the influence of tidal circulation on sediment transport in mangrove fringed creek systems. The study involved measurements of suspended sediment concentrations (SSC), salinity, temperature, current velocities and sea levels both in the tidal channels and in the mangrove swamp forest. Long-term SSC, sea level and current velocities were measured with an Orbital Backscatter Sensor, MicroTide pressure gauges and a SD-6000 current meter respectively. A pressure gauge connected to a backscatter sensor was also used to measure SSC along the creek. In addition SSC were determined by filtering water samples drawn from different levels of the water column with a Hydrobios water sampler. Water temperatures and salinities were measured *in situ* using an Aanderaa Salinity-Temperature sensor.

The results show that the SSC is higher in the upper mangrove fringed creeks and lower in the frontwater zones bordering the Indian Ocean. The mean near surface SSC in the upper mangrove region is 0.16 g/l while that in the lower region is 0.03 g/l. Near bottom SSC (in the upper zone) were usually higher and reached 1.40 g/l. In the lower frontwater zones, the near bottom SSC was of the order 0.10 g/l. At the creek entrance, the mean tidal volume fluxes in spring and neap are 2233 m^3/s and 937 m^3/s respectively. The (near bottom) mean tidal suspended sediment fluxes in spring and neap are 1220 Kg/s and 400 Kg/s respectively. The tidal sediment flux during flood tide ranged from 460 to 1740 Kg/s as observed at a cross-section near the entrance of the creek. The ebb ones were much lower being in the range 330-690 Kg/s. Major resuspension of bottom sediments which raises SSC to values higher than 1.0 g/l, occurs only during flood tide at spring when the current velocities reach 1 m/s or more. The turbidity maximum zone (TMZ) with the highest SSC occurs in the upper middle region of the creek (Stn 3-6) where SSC is in the range 0.07-0.16 g/l. This zone coincides with the salinity maximum zone (SMZ) with salinity in the range 36-38 in the dry season.

Calculations using formulas for erosion and deposition within the main tidal channel for the period between 15 and 23 February, 1999 showed that erosion reach 6.0×10^{-4} $Kg/m^2/s$ while deposition reach 5.0×10^{-5} $Kg/m^2/s$. Erosion dominates during periods of high current velocities and deposition during periods of low current velocities which occur at low and high waters. A coarse comparison between total sedimentation and river sediment supply indicates that most of the riverborne sediments are trapped within the creek. In dry season with low sediment supply from the rivers, sediments are imported into the creek from Kipevu basin. Sediments re-suspended during spring flood tide enter the mangrove swamp where they are trapped due to the dense mangrove vegetation and sluggish current velocities of the order 0.05 m/s which cannot keep sediment particle in suspension. Mean SSC is less than 0.05 g/l in the mangrove swamp. Sedimentation rate in the mangrove swamp is of the order 250 g/m^2 per spring tide, corresponding to an accretion rate in the mangroves of the order 30 cm/100 years. This is higher than the estimated local sea-level rise of 22 cm/100 years, implying that Mwache mangrove swamp is keeping up in pace with sea level rise.

Table of Contents

1.0 INTRODUCTION

This study focussed on Mwache creek, one of the two tidal mangrove-fringed creeks in the upper zones of Port-Reitz creek (Fig. 1). The objectives of the study are three fold; (1) establish the patterns of transport of suspended sediments, (2) determine the patterns of water and sediment exchange between the mangrove wetland and the creek and, (3) examine the underlying basic hydrodynamic processes influencing the sediment transport. Previous research in Port-Reitz creek have concentrated mainly in the southern Port area and includes studies on waste disposal by Norconsult A.S (GOK, 1975) and numerical modeling of sediment deposition west of Kipevu (Grosskopf and Onyango, 1991). However, these studies excluded the tidal creeks and mangrove swamps in the upper region of Port-Reitz creek. This study paid special attention to the little understood upper mangrove wetlands consisting of Mwache tidal creeks and mangrove swamp forest.

Mangrove wetlands are unique complex systems comprising tidal creeks and mangrove forests. They form the boundary between the terrestrial and coastal marine environment and occur mainly in semi-enclosed tropical creeks that experience significant sea level variations and inundation by seawater as a result of oceanic tides. The mangrove ecosystem has several important functions. Among the most important is its function as a nursery ground for coastal fish and as a source of firewood, timber and poles for building. They are also known for their beneficial role on the sustainability of coastal ecosystems, since apart from leaching of organic and inorganic nutrients which also become available to other marine systems, dense mangrove forest vegetation also trap sediments and protect the shoreline from tropical storms and erosion. However, it is not known whether mangrove creeks export or import suspended sediments and hardly is there sufficient data which can enable one to decide with any certainty whether mangroves are opportunistic colonizers or they build their environment. There is also uncertainty concerning the fate of mangrove ecosystems in light of the unprecedented sea level rise and increased supply of terrigenous sediments from river basins.

Studies of sediment transport dynamics in tidal creeks are vital for coastal zone management as they provide data and information on the influence of sediment load on mangrove ecosystems. Since a large component of the sediment load may be associated with anthropogenic activities at river basin level, by studying sediment transport processes, it is possible to identify factors stressing mangrove ecosystems and therefore enable appropriate and specific management actions to be devised. It is essential to establish periods when the mangrove creeks import or export suspended sediments and how the tidal dynamics influences the suspended sediment transport and dispersion in tidal channels as well as in the mangrove forest swamp. This information is vital to coastal scientists and natural resources managers interested in establishing factors that determine both long and short-term sustainability of the mangrove ecosystems.

Information on sediment transport dynamics in mangrove creeks is however not readily available in view of the limited number of studies specifically focused on mangrove wetlands. While a wealth of literature exists on salt-marsh sediment transport processes (Althausen and Kjerfve, 1992; Leonard *et al.*, 1995; Vogel *et al.*, 1996 and Smoak and Patchineelans, 1999), the same cannot be said for mangrove tidal creeks. However it is important to note that salt marshes are structural different from tropical mangrove complexes and there are also salient differences in the patterns of sediment transport. Similarly, studies have been conducted on estuarine sediment transport dynamics in the recent past (Wellerhaus, 1981; Althausen and

Kjerfve, 1992; Poulos and Collins, 1994; Uncles, *et al.* 1994; Lindsay *et al.*, 1996; Wolanski *et al.*, 1995; Wolanski *et al.*, 1996 and Saad *et al.*, 1999). But their results cannot be generalized for mangrove creeks since mangrove vegetation modify the sediment transport patterns. Few studies demonstrating the coupling between hydrodynamics and sediment transport in mangrove creeks have been conducted in Southeast Asia (Furukawa *et al.*, 1997, Wolanski *et al.*, 1995, Saad *et al.*, 1999), but these were mostly in mangrove creeks receiving substantial river supply of freshwater and sediments. These are thus different from Mwache creek which receives river freshwater and sediments for only a short period during rainy seasons (Kitheka, 1996).

Among a wide range of factors influencing sediment transport in tidal creeks, tidal range and current speed are the most important (Althausen and Kjerfve, 1992; Lindsay *et al.*, 1996). Channel erosion and deposition are dependent on certain critical velocities, which vary from place to place depending on the nature of tidal channel geometry and type of sediment. It has been reported that resuspension occurs during accelerating currents and deposition with decelerating currents (Uncles *et al.*, 1994 Wolanski *et al.*, 1996). However there are certain complications due to channel morphology as well as the effects of wind and river discharge so that the above generalization don't always hold water. It is often argued that in creeks with tidal asymmetry (Wolanski *et al.*, 1980, 1998a; Mazda *et al.*, 1995), the net sediment flux follow the pattern of the dominant tidal current. If the creek is ebb dominant, there will possibly be ebb dominance in the fluxes of suspended sediment (Aldridge, 1997; Lindsay *et al.*, 1996). However this may not always be the case. For example, Gao *et al* (1990) showed that tidal exchange, in the form of either vertical residual circulation or bay-mouth water mixing is responsible for the net landward movement of suspended sediment though the ebb currents may be stronger than the flood currents. Although Gao *et al.*, found tidal asymmetry not to be crucial in determining the direction of net transport of sediments, Aldridge (1997), Wolanski *et al.*, (1980, 1998b) and Mazda *et al.*, (1995) found the net sediment transport to be principally controlled by the asymmetry between flood and ebb tides. It is however debatable whether these results are applicable to mangrove creeks since there are mostly for bays and estuaries with no mangrove forests. In this study, results are presented on some aspects of sedimentation dynamics with particular emphasis on the influence of water exchange and resuspension-deposition dynamics on sediment fluxes as induced by varying magnitudes of tidal current velocities related to neap-spring tidal cycles.

1.1 *Literature review*

There have been a number of studies on tidal mangrove wetlands in the past. Quite a good number of these deal with hydrodynamics and sediment transport processes (Wolanski *et al.*, 1980; Furukawa *et al.*, 1997; Furukawa and Wolanski, 1996; Wolanski *et al.*, 1996, Wolanski *et al.*, 1998b). In the recent past there has also been an effort towards understanding sediment accretion processes in the mangrove swamp forests as it has been demonstrated by Ayukai and Wolanski (1997), Saad *et al.*, (1999) and Smoak and Patchineelam (1999).

Wolanski *et al.*, (1998a), working on the mangrove fringed Fly River, Papua New Guinea noted that mangroves traps 6% of the riverine sediment inflow and about ¼ of the riverine clay inflow. SSC fluctuates with the tide so that when the tidal range is less than 2 m, there is negligible resuspension of the bottom sediment. The SSC were high, exceeding 15 Kg/m^3 near the bottom and 8 Kg/m^3 at mid-depth of the water column. At such high concentrations, Wolanski *et al.*, (1998a) observed that the settling velocity of river sediments varied non-linearly with sediment concentration. The study found that the bulk of transport of

suspended sediment occurred mainly during a few days each month at maximum tidal range; a difference of only 0.2 m even in the high tidal range made a large difference to SSC. Wolanski *et al.*, noted that the erosion and settling of particles fluctuated from channel to channel, varying also with tides and wind. SSC fluctuated with the tidal currents, with the largest SSC prevailing at peak tidal currents and the smallest SSC at slack tide. Similar observations were made by Uncles *et al.*, (1985). Peak SSC values were observed to be generally higher at flood tidal currents than at ebb tidal currents and this was attributed to the asymmetry of tidal currents. Wolanski *et al.*, (1998a) concluded that time-series of depth-integrated fluxes of fine suspended sediment were strongly dominated by the tides.

Ayukai and Wolanski (1997) investigated the importance of biologically mediated removal of sediments from the Fly River plume, Papua New Guinea and reported SSC in the order 0.05 g/l inside the turbid water mass. They noted that SSC was rapidly reduced to a few milligrams per litre in the area where salinity was still as low as 26. Rapid removal of sediments from the plume was attributed to physico-chemical flocculation.

Althausen and Kjerfve (1992) reported that SSC depends largely on the tidal stage and varies significantly from spring to neap. Spring SSC is 2-3 times greater than concentrations during neap. Lindsay *et al.*, (1996) found that on the semi-diurnal time-scale, SSC are closely related to current velocities. In the near bottom waters, the current velocities required to make resuspension and deposition evident are 0.6 and 0.3 m/s respectively. Within the semi-diurnal tidal cycle, these velocities are exceeded for longer periods when the tidal range is large, so that spring cycles dominate in controlling the transport of suspended matter. Consistent with findings of Wolanski *et al.*, (1998a) and Althausen and Kjerfve (1992), Lindsay *et al.*, (1996) also noted that estuarine SSC are influenced by the tidal range and consequently often vary on semi-diurnal, fortnightly and seasonal time-scales.

Studies on sediment transport in estuaries shows that there exists the turbidity maximum zone (TMZ) in certain locations of the estuaries which are characterized by high SSC (Wellerhaus, 1981; Uncles *et al.*, 1985;Wolanski *et al.*, 1995). Wellershaus (1981) reported that TMZ occur in both estuarine and non-estuarine environments. A variety of explanations have been proposed for its existence. In case of non-estuarine circulation, the collection and subsequent sedimentation of particles with low settling velocities in the salt wedge area was found to be an important process by Wellershaus (1981). It is thought that this selection of particles is the main cause for the mud character of the sediment in the TMZ. On the other hand, tidal oscillation can also cause alternating sedimentation and resuspension of the particles with the latter been thought to be the main source of the visible turbidity maximum as reported in Uncles *et al.*, (1985). According to Wellershaus (1981) complicating factors in the formation of TMZ are the occurrence of a range of particles with different settling velocities, the removal of sediment by extraordinary forces like storms and human activities like dredging. Uncles *et al.*, (1994) pointed out that the TMZ may be due to local resuspension of cohesive bed sediment since TMZ is also found in estuarine systems where there is no convergence of currents near the channel bottom.

Geyer (1993) using a simple numerical model demonstrated that the reduction in turbulence due to stratification greatly enhances the trapping of suspended sediment that occurs at the estuarine turbidity maximum. According to Geyer (1993) the reduction of the turbulent diffusion can result in a reduction in the quantity of sediment that can be carried by the flow and this causes sediment to be trapped near the landward limit of the salinity intrusion. This trapping occurs at the same location as the estuarine convergence, but it seems to be more effective at

trapping silt-size particles. Uncles *et al.*, (1985) attributes the formation of TMZ from the tidal pumping of suspended sediment directed up-estuary near the head at spring tides. He argued that during spring tides, tidal pumping of sediment was much larger than transport due to vertical shear.

Within mangrove-fringed estuaries, Wolanski *et al.*, (1995) and Wolanski *et al.*, (1998a) reported that the turbidity maximum exists only at spring during which near-bottom SSC is greater than 5 g/l and occasionally exceeded 30 g/l. Wolanski *et al.*, (1995) concurred with Uncles *et al.*, (1995) by showing that the formation of the turbidity maximum zone is due to the simultaneous occurrence of tidal pumping and the baroclinic circulation. According to Wolanski *et al.*, (1995) the dominant mechanism influencing the variability of SSC is the tidal velocity, with alternating tide-locked periods of erosion and sedimentation. Wolanski *et al.*, (1998b) working in the mangrove-fringed Mekong river estuary, also noted that the asymmetry of tidal currents along with the baroclinic circulation, pump sediment upstream and this leads to the formation of the turbidity maximum. SSC values near the salinity intrusion limit, vary at tidal frequency with the depth averaged SSC peaking at 0.058 g/l and maximum near-bottom SSC values reaching 1.40 g/l.

In open marine marshes, it has been reported that total SSC and sediment load are also modulated by spring-neap cycle and time-velocity asymmetries in the tidal currents (Leonard *et al.*,1995). This finding is also consistent with the findings of Wolanski *et al.*, (1998a) working in mangrove fringed estuaries in Southeast Asia. However, Gao and Collins (1994) have noted that in an inlet system which has reached its equilibrium, it is not the current speed which determines the intensity of sediment transport through the entrance, but the intensity of sediment supply which also inadvertedly controls the current speed. As it has been shown in mangrove fringed estuaries (Wolanski *et al.*, (1998a), in salt marshes, there are also large neap-spring cycle in SSC (Leonard *et al.*, 1995). Spring SSC range from 0.005 to 0.04 g/l, whereas during neap, typical concentrations range from 0.005 to 0.01 g/l (Leonard *et al.*, 1995). Leonard *et al.*, have also shown that there are also great deal of variability in sediment flux in salt marshes and net suspended sediment loads are generally associated with smaller tidal prisms (e.g. neap tides) and larger net loads with larger tidal prisms (e.g. spring tides).

Wolanski *et al.*, (1996) reported that SSC in the Mekong River estuary (Vietnam) also vary with the tidal cycle and is higher near the bottom where it reached 0.6 g/l at peak ebb currents. Wolanski *et al.*, reported a background SSC of 0.15 g/l that is comparable to that of Lindsay *et al.*, (1996) of 0.20 g/l at Forth Estuary, Scotland. Wolanski *et al.*, (1996) also noted that, in the high flow season, sediments are deposited and eroded periodically with the tides in the freshwater region, but are still transported down-river at mean velocities of 0.5-1.0 m/s. Further it was shown that sediment exported to coastal waters during the high–flow season becomes available for entrainment into some estuaries during the low-flow season. Good example is in case of Mekong estuary (Wolanski *et al.*, 1996).

Thus, while a number of studies have been conducted on sediment fluxes and hydrodynamics, it is important to note that most of them have concentrated on non-mangrove environments. Most of the studies have been conducted in estuaries with high inflow of freshwater and terrigenous sediments. Very few studies have been conducted in mangrove wetlands of similar dimensions as Mwache creek which principally receive sediments from river basins only on seasonal basis. These creeks portray a combination of estuarine and non-estuarine circulation patterns. These rare types of mangrove wetlands are found along the semi-arid coast of East Africa and little is known as to their sediment transport dynamics. In such

creeks, it is expected that sediment transport processes in rainy season are different from those during dry season when river discharge is absent. While in rainy season such systems behave as estuaries for a relatively short period, the same cannot be said to be true during dry season when they function partly as evaporation basins. Thus sediment transport processes may be more complicated than in normal, freshwater dominated estuaries and open bays.

2.0 DESCRIPTION OF MWACHE CREEK

Mwache mangrove wetland occurs in the upper parts of Port-Reitz Creek (04° 03 S and 039° 38 E), one of the two main tidal mangrove-fringed creeks found in the Mombasa District, Kenya (Fig.1). It has been postulated that the flooding of the coastal river valleys as a result of sea-level rise (Caswell, 1956) during Holocene era may have lead to the formation of the creek. The total creek surface area determined from a topographic map (East Africa 1:50,000; Sheet 201/1, Series Y731, Edition 5-SK, 1973) was estimated to be 17 Km^2. The mangrove forest cover an area of 12 Km^2, which is roughly 70% of the total area of the creek (Table 1). The length of the Mwache creek from the entrance to Kipevu basin is approximately 12 Km. The main tidal channel is shallow. At spring high waters the depth is less than 14 m deep at the creek entrance to Kipevu basin and less than 6 m in the upper zones fringing the mangroves (Fig.1). Tidal creeks meander through the wetland cutting the soft Jurassic shales and sandstone rocks (Caswell, 1956) which rises approximately 120 m above the creek low water level. The mangroves in the upper parts fringe the lush tropical lowland forest formed on uplifted sandstone massif through which Mwache River has cut deeply on its way to the creek. In the lower region East of Kipevu, some sections have been dredged and water depths in the order of 20 to 35 m are encountered.

The air temperature varies from the minimum of 24^0C in July to the maximum of 32.5^0C in February. The total annual rainfall shows great interannual variability with mean values in the order of 900 mm. In certain years as in 1997, total annual rainfall may be high due to abnormal rainfall and temperature conditions associated with *El Nino* phenomena as shown in Fig. 2. Annual evaporation is in the order 1800 mm which is much higher than normal annual total rainfall with the result that there is a freshwater deficit in dry seasons in the basin. The water circulation is mainly driven by semi-diurnal tides but there are also effects of wind and river discharge, although their magnitudes have not been established. The creek receives freshwater and terrigenous sediments from two seasonal rivers namely, Mwache and Mambome. Their mean discharges and basin areas are shown in Table 2. The total catchment area of the two rivers draining into Mwache creek is 2600 Km^2. Mwache River with a catchment area of about 1700 Km^2 is one of the largest with freshwater discharge below 10 m^3/s in normal rainfall months. During normal rainfall years, it is estimated that the input of terrigenous sediments is of the order 7×10^4 ton/year (Table 2) but the input increases almost tenfold in periods associated with above normal rainfall (Kitheka, 1996). A general survey on the spatial distribution of different species of mangroves showed that, the dominant species are *Avicenia marina* and *Rhizophora mucronata.* These species are usually found fronting the tidal creeks. In the middle zones of the mangrove forest occurs a mixed stand of *Rhizophora mucronata* and *ceriops tagal.* In the inner zones bordering the dry land occurs mainly *Ceriops tagal* species. GOK (1975) subdivided the creek according to the most beneficial uses. The present main socio-economic activities in the upper zones include mangrove harvesting,

artisanal fishing and subsistence farming (Daily Nation, 30/6/99). The Port of Mombasa, one of the largest in Eastern Africa, is located in the lower zones.

3.0 MATERIALS AND METHODS

3.1 *Sampling stations*

The sampling stations shown in Fig. 1 were established in the lower, middle and upper regions of Mwache creek. The principal stations were Stns 1, 6 and 8. Stn 1 is located at the Mwache estuary in the upper region, while Stn 8 is located at the shallow Kipevu basin. Stn 6 located at the middle lower section of the creek was used as the principal station for time–series measurements. For gauging of the effect of oceanic flows, Stn 10 located at the entrance of Port-Reitz creek to the Indian Ocean was established as a control station.

3.2 *Determination of sediment concentration*

SSC were determined using two approaches which are; (1) gravimetric and (2) automated approaches (Dyer, 1979; McGave, 1979;Vogel *et al.,* 1996). In the first approach, water-sediment mixture samples were drawn from the surface, middle and bottom water columns using a hydrobios water sampler. Samples were filtered in the laboratory using pre-weighed 47 mm Whatman GF/C filters with 0.45 μm pore diameters. Salts were flushed from filtered samples using distilled water after which they were wrapped in aluminum foil and then dried in oven at 120°C for 24h. They were then re-weighed to determine the weight of filtered sediments, which was taken as the difference between the weight of the filter with the filtrate and the original weight of the filter. This was then related to the filtered volume of seawater to determine SSC as the amount of sediments present in a filtered volume of seawater. In the second approach, Orbital Backscatter sensor (OBS) connected to a MicroTide pressure gauge was moored at a central location of the channel at Stn 6 and used to measure SSC automatically. The instrument was programmed using a portable computer and logged in SSC at an interval of 5 min in the period between January 26-30 and between February 2-23, 1999.

3.3 *Physical variables and sampling strategy*

Both spot sampling and automated continuous time-series measurements were implemented for salinity, temperature, tidal current velocities and sea level. Spot surveys were carried out twice a month from a rubber dinghy in the period between March 1998-March1999. The sampling cruise with a boat from Stn 1 to 8 took 45 min to 1 h. Stn 6 was chosen as the principal station for instrumented time-series measurements in view of its accessibility and availability of adequate security which is necessary in regard to the mooring of the MicroTide pressure gauge and SD-6000 rotor current meter.

The time series measurements for salinity, temperature, SSC, tide and current velocities were conducted at Stn 6 on August 14-15 (spring), July 29-30 (spring), November 12-13 (neap) and October 9-10 (spring), all in 1998. In these time-series campaigns, the above variables were measured at an interval of 1 h for periods ranging from 12 to 25 h which essentially covered 2-4 tidal cycles (summarized data in Table 8). Water salinity and temperature were measured using an Aanderaa Salinity-Temperature meter. Vertical velocity profiles were also determined for

different stages of the tide at Stn 6 using Pendulum current meters (Cederlof, *et al.,* 1996). Other sets of time-series measurements were carried out using an automated instruments in which current velocities, temperatures, SSC and sea level variations were logged at 5 min interval at Stn 6 using an SD-6000 current meter and MicroTide pressure gauge respectively. A MicroTide pressure gauge connected to an Orbital Backscatter Sensor and a SD-6000 current meter were moored at the central location of the channel, about one meter above the channel bed in the period between January 26-30 and February 2-23, 1999. These measurements covered both neap and spring tides.

Mwache creek has not been surveyed and information on bathymetry was not available. Thus, in the period between February 24 and 25, 1999, an intensive campaign on water depth measurements was implemented in the creek. Depths were measured at every 10 m point with a hand-held Echo Sounder in transects located 50-100 m apart. The measured depths were corrected for tides using the tidal prediction tables (Magori, 1999) to produce the bathymetric chart of Mwache creek as shown in Fig. 1. This was then used together with time-varying sea level and cross-sectional area at Stn 6 to construct the hypsometric curve of the creek, which was in turn used for computing volume fluxes and current velocities in the creek.

3.4 *Determination of sedimentation patterns in the mangrove swamp*

In order to investigate the relationship between SSC and flow velocities in the mangrove forest, several transects extending 70 to 450 m into the swamp were established perpendicular to the creek channel according to an approach similar to that used by Furukawa *et al.,* (1997). Along these transects, water-sediment mixture samples were taken at mid-depth at high tide when water covered the mangrove wetland to a level of approximately 0.1 m in the upper reaches and about 1.0 m in the lower reaches fronting the main tidal channel. Samples were carefully collected at an interval of 10 m from the creek channel bank, upto the landward limit of the swamp. At the central position along the transect, several time-series measurements on tidal elevation, flow velocities and SSC were undertaken at an interval of 10 to 15 min for 2 to 4 h. This covered both flood and ebb periods in spring. Water level in the mangrove wetland was measured with a tide pole and currents with small floats since a rotor current meter could not be used due to dense mangrove vegetation and extremely low current velocities encountered. SSC were then determined in the laboratory using the filtration procedure outlined earlier.

3.5 *Data treatment and analysis*

The collected data were subjected to statistical analyses using Matlab computer software. Analyses of interest included among others, measures of central tendency (mean, standard deviation), correlation and regression analyses (Steel and Torrie, 1981). These were supplemented with other analyses based on hydrodynamic principles such as harmonic analysis. For statistical data with observations $x_1, x_2, x_3, \ldots x_N$ the mean was computed as

$$\bar{x} = \frac{x_1 + x_2 + \ldots\ldots + x_n}{N} = \frac{1}{N}\sum_{i=1}^{N} x_i \qquad (1)$$

And for statistical data with observations $x_1, x_2,\ldots,x_N$ the standard deviation (s) was defined as follows according to Rade and Westergren (1990)

$$s^2 = \frac{1}{N-1}\sum_{i=1}^{N}\left(xi - \bar{x}\right)^2 \tag{2}$$

The correlation analysis was based on the calculation of correlation coefficient (r) using the Equation given in Steel and Torrie (1981) which is written as

$$r = \frac{\sum\left(X-\bar{X}\right)\left(Y-\bar{Y}\right)}{\sqrt{\sum\left(X-\bar{X}\right)^2}\sqrt{\sum\left(Y-\bar{Y}\right)^2}} \tag{3}$$

The correlation coefficient (r) lies between +1 and –1 with the former and the latter implying perfect positive and perfect negative correlation respectively. In case there is no relationship between independent and dependent variables, the correlation coefficient (r) is zero (Steel and Torrie, 1981).

3.6 *Harmonic analysis of sea level record*

Harmonic analysis was used in the determination of tidal constituents as well as separation of the sea level record into tidal and residual components. The analysis was done following a Matlab program developed by Cederlof (1998). Given a time series $Z(t)$ of sea level data, its tidal part is expressed as a combination of sine and cosine functions so that

$$Z(t) = \sum_k a_k \sin(\omega_k t) + \sum_k b_k \cos(\omega_k t) \tag{4a}$$

k=1,2...k

The values of a_k and b_k can be calculated for k given frequencies ω_k by minimising the sum of squares of the differences between the assumed function and the given sea level time series Z_n. The least squares fit require that

$$f(a_i, b_i) = \sum_{n=1}^{N}\left(Z_n - \sum_{k=1}^{k} a_k \sin(\omega_k t_n) + \sum_{k=1}^{N} b_k \cos(\omega_k t_n)\right)^2 = \min imum \tag{4b}$$

This requirement is satisfied if

$$\frac{\partial f}{\partial a_i} = 0$$

$$\frac{\partial f}{\partial b_i} = 0$$

$$i = 1, 2, 3, K$$

Where

$$\frac{\partial f}{\partial a_i} = -2\sum_{n=1}^{N} \sin(\omega_i t_n)\left(Z_n - \sum_{k=1}^{k} a_k \sin(\omega_k t_n) - \sum_{k=t}^{k} b_k \cos(\omega_k t_n) \right) = 0 \tag{4c}$$

and

$$\frac{\partial f}{\partial b_i} = -2\sum_{n=1}^{N} \cos(\omega_i t_n)\left(Z_n - \sum_{k=1}^{k} a_k \sin(\omega_k t_n) - \sum_{k=t}^{k} b_k \cos(\omega_k t_n) \right) = 0 \tag{4d}$$

The Equations 4c and 4d are then written as

$$\sum_k a_k \sum_{n=1}^{N} \sin(\omega_k t_n)\cos(\omega_k t_n) + \sum_k b_k \sum_{n=1}^{N} \sin(\omega_i t_n)\sin(\omega_k t_n) = \sum_{n=1}^{N} Z_n \sin(\omega_i t_n) \tag{4e}$$

$$\sum_k a_k \sum_{n=1}^{N} \cos(\omega_k t_n)\cos(\omega_i t_n) + \sum_k b_k \sum_{n=1}^{N} \cos(\omega_i t_n)\sin(\omega_k t_n) = \sum_{n=1}^{N} Z_n \cos(\omega_i t_n) \tag{4f}$$

These are then simplified by introducing the notations

$$X_{ik} = \sum_{n=1}^{N} \sin(\omega_k t_n)\cos(\omega_k t_n) \qquad S_{ik} = \sum_{n=1}^{N} \sin(\omega_i t_n)\sin(\omega_k t_n) \qquad S_i = \sum_{n=1}^{N} Z_n \sin(\omega_i t_n) \tag{4g}$$

$$X_{ik} = \sum_{n=1}^{N} \cos(\omega_i t_n)\sin(\omega_k t_n) \qquad C_{ik} = \sum_{n=1}^{N} \cos(\omega_k t_n)\cos(\omega_{ki} t_n) \qquad C_i = \sum_{n=1}^{N} Z_n \cos(\omega_i t_n) \tag{4h}$$

$$\sum_k a_k X_{ik} + \sum_k b_{ki} S_{ik} = s_i \tag{4i}$$

$$\sum_k a_k C_{ik} + \sum_k b_k X_{ik} = c_i \tag{4j}$$

Equations 4g and 4j gives a system of $2K$ Equations in $2K$ unknowns; a_1 through a_K and b_1 through b_K. The F-ratio scale using the Form number $F=(K_1 + O_1)/(M_2 + S_2)$ was used to characterize the tide into semi-diurnal type (F=0.188) as is shown in Table 3. In the expression for computing Form number, K_1, O_1, M_2 and S_2 represents diurnal and semi-diurnal tidal constituents. The neap and spring tidal ranges were calculated using the main tidal constituents derived from harmonic analysis as shown in Table 4.

3.7 *Sediment Mass Transport*

The hypsometric curve of the Mwache creek was generated from the tide corrected bathymetric data. The creeks surface areas (A_j) at depth (h_j) were then determined and the total water volume (V_N) at depth h_N was calculated as

$$V_N = \sum_{j=1}^{N} A_j (h_{j+1} - h_j) \tag{5}$$

Since water depths change with time due to tidal forcing, the tidal volume flux $Q(t)$ was computed as follows according to Vogel *et al.*, (1996)

$$Q(t) = A(t)\frac{dh}{dt} \tag{6a}$$

With simultaneous corresponding data on instantaneous suspended sediment concentrations $C_o(t)$, suspended sediment flux $Q_s(t)$ was then computed as

$$Q_S(t) = Q(t)\, C_o(t) \tag{6b}$$

Tidal current velocities $U(t)$, were computed from the volume flux $Q(t)$ and vertical cross-section area $A_c(t)$ at Stn 6 as

$$U(t)=Q(t)/A_c(t) \tag{6c}$$

This method assumes uniform velocity distribution across the channel. Channel contraction coefficient was neglected because of large cross-sectional area at Stn 6. Similar approach for

computing volume and material fluxes as to the one applied in this study have been used elsewhere but with some modifications which are necessary in order to suit specific study areas. Good example include studies by Leonard *et al.*, (1995) and Lindsay *et al.*, (1996), although particular attention has been given to the application in salt marsh tidal creeks and estuaries.

3.8 *Flood and ebb volume fluxes*

Mean flood and ebb volume fluxes (Q_f and Qe) were computed according to the following Equation

$$Q_f = \frac{\Delta V_T}{T_f} \tag{7a}$$

$$Qe = \frac{\Delta V_T}{Te} \tag{7b}$$

Where ΔV_T is the tidal prism at mean sea level during spring. T_f and Te are the mean flood and ebb durations respectively. The product of surface area (A_o), and tidal range (R_f), yields the tidal prism (ΔV_T).

3.9 *Mean flood and ebb velocity*

The mean velocities during flood (U_f) and ebb (U_{eb}) tide at Stn 6 were calculated as

$$U_f = \frac{Q_f}{A_c} \tag{8a}$$

and

$$U_{eb} = \frac{Q_e}{A_c} \tag{8b}$$

Where A_c is the creek cross-sectional area at Stn 6 which is roughly 1750 m^2 if a water depth of 7 m and width of 250 m are assumed to be representative of spring conditions.

4.0 *Erosion and deposition of sediments*

The continuous time-series data on SSC and current velocities at Stn 6 extending from February 15 to 23, 1999 were used to estimate some empirical constants used for determination of erosion and sedimentation rates. The vertically-averaged sediment mass conservation equation (see Wolanski *et al.*, 1995) applied in a finite section of the channel is simplified as follows

$$\frac{\partial(HC)}{\partial t} = M_e - M_d \tag{9a}$$

In Equation 9a, H is the water depth, C is the depth averaged SSC and t is the time. The source and sink terms are erosion (M_e) and deposition (M_d). These are important components of the model and have to be determined separately. These terms are governed by specific critical velocities which were determined by examination of the simultaneous plots of SSC and current velocities. The deposition rate (M_d) was computed assuming

$$M_d = CWs\left(1 - \frac{U}{U_d}\right)^2; U < U_d$$

$$M_d = 0; U > U_d \tag{9b}$$

In above model, U is the bulk velocity; that is the velocity outside boundary layer, U_d is the critical velocity for settling and W_s is the sediment settling velocity (Dyer, 1979; Wolanski, *et al.*, 1995). The critical deposition stress (τ) is computed as

$$\tau = \rho C_d U^2 \tag{9c}$$

The source of SSC represented by erosion of sediments from the channel bottom (M_e) was calculated from

$$M_e = \alpha\left(\frac{U}{U_e}\right)^2 - 1 \tag{9d}$$

The Equation 9d is only applicable if the bulk current velocity (U) is higher than the critical erosion velocity (U_e). α is an empirical constant that can be related to critical shear stress since α is a function of τ/U_d. A value of α=0.00008 and computed shear stress, $\tau_d = 0.97 \times 10^{-3}$ were used for our calculations of erosion rates.

4. RESULTS

4.1 *Tidal characteristics and current velocities*

The tides measured at Stn 6 in the Mwache creek are purely semi-diurnal (F=0.188) with two low and high waters in approximately every 25 h. The sum of O_1 and K_1 tidal constituent amplitudes is less than 20 % of that of the sum of M_2 and S_2 (Table 4). The examination of the original and computed 22 days record of the tide shows that the residual oscillations are usually less than 0.15 m (Fig. 3). These shows water level changes contributed by atmospheric pressure variations and wind set-up are usually small as compared to those caused by tide. The neap and spring tidal ranges are 1.3 and 3.1m respectively as shown in Table 5. Spectral energy density analysis was carried out on sea level record in order to establish the dominant signal. Semi-diurnal tidal signal was found to dominate the record as shown in Fig. 4. The dominant low frequency signal approximates 12.30 h, which is typical of modulations caused by tidal forcing.

The examination of the tidal curve revealed some degree of asymmetry between flood and ebb period (Figs. 5, 6a-b and 7a-b) with slightly longer ebb tides and relatively shorter flood tide. The mean duration of flood and ebb tides determined by inspecting the 22 days sea level record are 6.20 and 6.60 h respectively. Associated with sea level variations are tidal currents (Figs. 5a-b, 6a-b) with neap-spring cycle as been reported previously in similar creeks by Leonard *et al.*, (1995), Prindle *et al.*, (1997) and Wolanski *et al.*, (1980). Within the creek entrance, maximum current speed is a function of the creeks' surface area and sea level variability. Using the 22 days sea level record and cross-sectional area variation at Stn 6 as a function of sea level, the tidal current velocities in the creek were computed using the equation 6c. These results, presented together with the plot of the semi-diurnal tide are shown in Figs. 7a-b. Comparison of measured and the computed current velocities shows that the two are largely similar with r value of 0.94 which is significant at 95% confidence level (Fig. 6a-b). There are however some minor differences in their features as the measured current velocities are more asymmetrical than the computed ones. This is probably due to lack of topographic details in the hypsometric curve (Fig. 8). The examination of measured current velocity pattern shows that, during spring, the asymmetry of the current velocities is high. This feature is however not very prominent in the calculated velocities. However, by considering their magnitudes, both computed and measured current velocities are of the same order of magnitude (Figs. 6a-b). The maximum current velocities at spring during flood and ebb are 1.25 and 1.38 m/s respectively and at neap, the maximum ebb and flood current velocities are 0.55 and 0.52 m/s respectively (Table 6). The difference between ebb and flood velocities are less than 0.15 m/s. These results indicate that Mwache creek is weakly ebb dominant, particularly when one considers both the magnitude of tidal current velocities and sea level patterns.

Table 6 also presents results from the computation of mean volume fluxes at ebb and flood tides during neap and spring. The spring high tide water volume at Mwache creek is approximately 60 x 10^6 m^3 while the spring low water volume is 20 x 10^6 m^3 when the depth change due to a 3 m tidal range is taken into consideration (Fig. 9). This yields a spring tidal prism (ΔV_s) of 40 x 10^6 m^3 which is equivalent to a tidal volume exchange of roughly 60% per tidal cycle at spring. The neap tidal prism (ΔV_n) is lower being 15 x 10^6 m^3 since the low and high water volumes are 13 x 10^6 m^3 and 28 x 10^6 m^3 respectively. The spring high water volume at creek is only about 18% of the total volume of water in Port-Reitz creek, since the total volume at the entire Port-Reitz creek during mean spring and neap is 341x10^6 and 153 x 10^6 m^3

respectively (GOK, 1975). Considering the high water surface area of the Mwache creek, the average tidal volume flux is estimated to be 2300 m^3/s. Since there is no significant sink or source of freshwater, the mean tidal volume fluxes of 2233 m^3/s and 937 m^3/s are assumed to be the most representative tidal volume fluxes in spring and neap tides respectively. These data are within acceptable limits given the assumptions in our calculations that sea level spatial variations upstream of the control Stn 6 are not significantly different.

4.2 *Temperature and salinity variations*

Time-series measurements of water temperature at Stn 6 (February 2-23, 1999) shows that, the temperature variations are mainly diurnal as is shown in Fig. 10. This finding is consistent with that of Hoguane *et al.*, (1999). Temperature rise and fall patterns are asymmetric with rapid rises during the day and gradual and relatively longer decrease in the evening and night. Maximum temperatures of between 30-31°C occur in the transitional periods between spring and neap tide and lowest in the order of 28-29°C occur during spring tide (Fig. 10). Based on monthly surveys conducted in different stations, the highest temperature occurs at the inner mangrove zones and there was a progressive decline towards the frontwater zone Stn 9. The lowest temperature (24.6°C) was recorded in July and the highest (31.50°C) occurred in February 1998. As at Stn 6, the lowest temperature (24.58°C) in the frontwater zone at Stn 10, also occurred in July and maximum (31.6°C) also in February. The standard deviations of temperature in all zones were of the order 2°C.

Figures 11 and 12 present vertical salinity and temperature profiles at different stations during periods of relatively high river freshwater supply and during dry season. It is evident in Fig. 11 that by June 1998 period there was still a significant effect of river freshwater supply into the creek after the cessation of the long-rains in April-May period as salinities were low (15-32) upto Stn 6. Salinities were mainly oceanic (>34.5) beyond Stn 8 with a progressive increase towards the open ocean. The upper Stns 1-4 in the Mwache estuary tended to portray some measurable stratification during periods of high freshwater supply.

The vertical salinity and temperature profiles done during relatively dry period in October 1998, showed a progressive increase in salinity towards Stn 1 at the estuary as shown in Fig 12. There was also a measurable stratification in the upper stations as high salinity water (36-37) is formed due to evaporation and evapotranspiration (see also Hoguane *et al.*, 1999). In both dry and wet seasons, stations located in the lower zones of the creek (Stns 7-8) showed uniform vertical distribution of both temperature and salinity, signifying well-mixed conditions (Figs. 11-12). In general the horizontal salinity gradient was positive in rainy seasons (+2.8/Km) and negative in dry season (-0.18/Km).

There is also a wide salinity variations at the inner mangrove stations (Stns 1-4) as compared to the frontwater zone. The standard deviation for salinity in the upper zone at Stn. 1 was of the order 10 while in the frontwater zone it was of the order 2 (Tables 7 to 11). The area between Stn 2 and 6 experienced relatively higher salinities (36-37) in dry season (Fig. 12). This region was regarded as the salinity maximum zone (SMZ). Its existence as a persistent feature in dry season was attributed to be due to evaporation and evapotranspiration.

Between March 1998-February 1999, salinity at Stn 1 varied from 1.5 to 36.4 implying a monthly rate of salinity increase of 3.2/month. In the lower zone at Stn 9, salinity varied from 29.4 to 36.2 in the same period implying a rate of change of 0.75/month. Thus, although there

are no major vertical salinity gradients in the creek, the horizontal salinity gradients could be significant to the extent of influencing sediment particle flocculation processes.

4.3 *Zonal SSC variations and gradients*

Seasonal and neap-spring SSC variations (Tables 10-12) were noted for the inner mangrove zones (Stns 1 and 6) as compared to the stations located in the frontwater zone (Stns 9 and 10). To a large extent, the SSC variations presented in this thesis cannot be largely attributed to the river discharge since in 1998-1999 period, drought prevailed and there was no significant supply of terrigenous sediments from the river basins. The seasonal river discharges were often less than 0.05 m^3/s. Moreover, river water SSC were lower (<0.04 g/l) than that in the creek.

Fig. 13 shows the SSC variations along the length of the creek at stations located above Stn 8. The measurements were done about 2 hours after low water spring (LWS). As shown in this contour plot, there is evidence of resuspension and advection of sediments from the channel bottom to the surface water column in the region between Stn 3 and 7. Higher SSC occurs in the lower 1 to 3 m of the water column near the channel bottom implying that, the water column is stratified during low waters when deposition dominate. The water column is partially well mixed during high tide (not shown). Considerable anomalies in the pattern of vertical distribution of SSC occur during periods of high current velocities due to turbulence. Our data indicate that highly turbid water is usually resuspended into the surface and middle water columns from the channel bed during flood tide as shown in Fig. 13. This could be attributed to strong currents in the zone between Stns 3 and 7 because of the relatively narrow and shallow channel cross-sections. The patterns of SSC as shown in Fig. 13 represent a balance between downward settling of suspended particles (CW_s) and upward turbulent diffusion $\kappa_t(\partial C/\partial z)$ associated with resuspension.

A turbidity maximum zone (TMZ) with the highest SSC was found mainly in the region between Stn 3 and 7 (Fig. 13). The SSC in this zone is in the range 0.10-0.16 g/l. This zone roughly coincided with the salinity maximum zone (SMZ) and it is not clear as to whether formation of the salinity maximum by evaporation is in any way connected to the formation of the turbidity maximum. This is a matter deserving further investigation. However since maximum tidal current velocities of the order 1.0 m/s were also measured in this zone, it is tempting to attribute the formation of the turbidity maximum to the resuspension of the bottom sediments by strong currents as is demonstrated in Fig.14a-b. The TMZ is a dynamic feature in terms of both its intensity and location, as it shifts positions so that during ebb tide it moves towards Stn 7 and during flood tide it moves further upstream towards Stn 3 in the precincts of the Mwache estuary. By further considering the spatial distribution of SSC, one notes a significant SSC spatial gradient. In general, the SSC in the frontwater zones were more than 50 % lower than those in the mangrove-fringed creeks. The concentrations declines drastically towards the open ocean, an observation which is consistent with that of GOK (1975) which reported increasing turbidity inwards during the southeast monsoon. The inner mangrove stations were also characterised by relatively large standard deviations of SSC as compared to stations in the frontwater zones (Tables 7 to 12). In the period between March 1998 and March 1999, SSC at Stn 1 varied from 0.019 g/l to 0.90 g/l with a mean of 0.163 g/l. The near bottom SSC at Stn 1 was often of the order 1.40 g/l. At Stn 6, near surface SSC during the same period ranged from 0.011 to 0.08 g/l with a mean of 0.033 g/l while those at the lower region (Stn 9)

ranged 0.011-0.073 g/l with a mean of 0.022 g/l (Table 7). This gives a positive inward longitudinal suspended sediment gradient of the order 0.014 g/l/Km implying an increase in SSC in the inner mangrove zones of the creek. In most stations, near bottom SSC was approximately 50% higher than the near surface one and was often above 1.0 g/l.

4.4 *Velocity-induced sediment re-suspension*

Figs. 14a-b shows the connection between sea level, tidal current velocities and SSC at Stn 6 in February 1999. Based on these observations, there is clear evidence of increased SSC during flood tide and a rapid decline during ebb tide. This observation is consistent with resuspension patterns demonstrated by contour plot shown in Fig. 13. The rapid increase in SSC during flood tide is followed by a rapid decline during ebb possibly because most of the suspended sediments are trapped in the mangroves so that during ebb, only a small quantity is available for transport toward Kipevu basin (Fig. 14a-b). Periods of major bottom sediment re-suspension are associated with maximum spring current velocities in the order of 1.0 m/s or more. Since the magnitude of tidal current velocities declines at neap tide, there is also a corresponding reduction in the magnitude of SSC during neap. By further considering Fig. 14a-b, it is also evident that resuspension varies with tidal elevation so that maximum SSC appears when the tidal elevation is greater than ±1.5 m. These are periods associated with spring tides as well as maximum current velocities of the order 1.0 m/s. For neap tidal elevation less than ±1 m, there is less resuspension since such lower tidal elevations are associated with non-erosive current velocities less than 0.50 m/s. By further considering Fig. 14a-b, one notes a general increase in mean SSC toward neap, which can be attributed to the presence of suspended sediment of finer particle sizes as compared to those resuspended in spring. However the highest and lowest SSC occur in spring. During neap, SSC variations tends to be moderate which in the long-run gives mean SSC of the same order of magnitude as high as that in spring. However, it is also important to note that the spring SSC as shown in Fig. 14a-b could be higher than 1 g/l since the latter was set as the threshold of the Orbital backscatter sensor. The high spring SSC in the creek could be an indication of trapping. In general there is a tendency for SSC to increase as current velocities increase (Figs. 20 and 21) which is expected since higher velocities induce turbulence which is necessary for resuspension of bottom sediments of different particle sizes.

4.5 *Suspended sediment fluxes*

By using the ebb and flood differences between the lowest and highest SSC in spring and neap as shown in Figs. 14a-b and, by considering their respective mean tidal discharges, it was possible to compute suspended sediment fluxes in neap and spring. These computations show that there are differences in the suspended sediment fluxes in neap and spring as shown in Table 6. The suspended sediment flux is in the order of 1700 Kg/s in spring and 500 Kg/s in neap, a difference of roughly 70%. These fluxes correspond to higher tidal volume fluxes in spring than those in neap. Despite ebb dominance, the flood sediment fluxes are higher than ebb ones in both neap and spring (Fig. 15). The integration of ebb and flood tide sediment fluxes over time shows there is a net import of sediments into the creek (Fig. 16a-b). The mean spring ebb sediment flux is 690 Kg/s as compared to flood flux of 1740 Kg/s. In neap, mean ebb sediment flux is 340 Kg/s while that of flood is 460 Kg/s. The difference between neap flood-

ebb fluxes is +120 Kg/s, while that in spring is +1050 Kg/s. The dominance of flood sediment flux is also consistent with our data on SSC and tidal current velocities as shown in Fig.14a-b. The dominant flood tide resuspension of bottom sediments explains the integrated sediment mass flux over the entire creek of the order 80,000 tonnes (Fig. 16a-b). These sediment fluxes are also related to the erosion-deposition cycles as shown in Figs. 18a-d. Deposition occurs in periods of sluggish currents during high and low waters, and erosion during periods of peak current velocities, about 2-3 h after high and low waters (Fig. 18a-d). The rates of erosion reached 6.0×10^{-4} Kg/m^2/s and those of deposition reached 5.0×10^{-5} Kg/m^2/s implying that the erosion is at least 10 times higher than the deposition. Since the critical velocities for erosion and deposition vary throughout a tidal cycle, there are also temporary variations in the intensity of erosion and deposition in a tidal cycle.

4.6 *Effective particle settling velocity*

The relationship between SSC and settling velocity determined using seawater of salinity of 35 showed an existence of a non-linear relationship between the two as shown in Fig. 19. The relationship is quite strong with the coefficient of determination (R^2) of 0.87 significant at 95% confidence level. Settling velocities were in the range 0.0004-0.001 m/s with the typical mangrove swamp settling velocity of 0.0005 m/s falling in the lower limits. The settling velocities are higher at lower SSC and lower at higher SSC, possibly because of the presence of a wide range of particles of different sizes at high concentrations. The results of particle size determination based on sieve analysis showed that, 50% of the sediment particles are in the range 90-180 μm which is typical of silt and very fine sand particles. The corresponding settling velocity should be of the order 0.0005 m/s (cf. Poulos and Collins, 1994; Furukawa and Wolanski, 1996). In seawater, settling velocity tends to be high because salt leads to the formation of particle flocs that because of their weight tend to settle faster. Furukawa and Wolanski (1996) have shown that the settling velocity of sediment particles in freshwater based on Stokes law, are of the order of 0.00008 m/s in the absence of flocculation.

Poulos and Collins (1994) have estimated typical sediment particle settling velocities for sediment particles of different sizes. For very fine sand and silt, they found settling velocity to range 0.0003-0.007 m/s which is consistent with our results. Similar results have been reported by Lund-Hansen *et al.,* (1994) who found the settling velocity for silt to be in the range 0.0001-0.0005 m/s. In mangrove creeks, Furukawa and Wolanski (1996) reported a settling velocity of 0.0005 m/s.

Based on our results as well as the results of the previous research conducted elsewhere (Lund-Hansen *et al.*, 1994; Poulos and Collins, 1994 and Furukawa and Wolanski, 1996), a settling velocity of the order 0.0005 m/s was found to be more representative of the Mwache creek sediments. This rate was used in our calculations of sedimentation in the mangroves.

4.7 *Calculation of eddy diffusivity from vertical SSC gradient*

Earlier, it was shown that resuspension depends on tidal range and magnitude of the tidal currents. A parameter associated with current velocities is the shear stress. Attempts were made to estimate its magnitude in the Mwache tidal creek. Changes in bottom shear stress are related to the vertical velocity gradient. This influences the rate at which sediment particles at the channel bed are advected into the water column. The estimation of this parameter is therefore of importance in understanding the patterns of resuspension of the bed sediments. In

the determination of the influence of eddy diffusion and shear stress, the vertical distribution of velocities at Stn 6 was analyzed and used to estimate the bottom shear stress (τ_c) as a function of the mean current velocity (U) using the following Equation

$$\tau_c = \rho U_*^2 \tag{12}$$

where ρ is the water density and U_* is the mean bulk current velocity above the bed measured with the Pendulum current meters. This yields a typical bottom shear stress (τ_c) of the order 0.9 N/m^2. Considering the magnitude of current velocity used in our calculation, this is certainly a relatively high shear stress which could have an important implication on the resuspension of bottom sediments since higher shear stress generates more turbulence. Bottom shear stress of the order 0.1 N/m^2 was reported from Old Tampa bay, Florida (Schoelhamer, 1995). In a recent study, Manning and Dyer (1999) have shown that increasing turbidity at low shear levels encourages floc growth, but the effect of the increasing turbulent shear together with increasing concentration in suspension causes disruption rather than enhancing the flocculation processes. The erosional behaviour of the mud water interface probably results from strong shear stress, which resuspends sediments and maintain a balance with downward particle settling.

The vertical distribution of SSC during high water in both neap and spring was used to calculate the eddy diffusivity (A_z). A balance between downward flux of SSC and upward flux is assumed to be due to mixing so that

$$A_z \frac{\partial C}{\partial z} = W_s C \tag{13}$$

The maximum eddy diffusivity (A_z) computed using Equation 13 is of the order 170 cm^2/s at current velocity of about 1.0 m/s during spring and is of the order 60 cm^2/s at current velocity of 0.30 m/s during neap. The $\partial C/\partial z$ range from 0.001 to 0.004 g/l/m. In Aarhus bay in the SW Kattegat, Lund-Hansen *et al.*, (1994) reported eddy diffusivity (A_z) upto 47 cm^2/s. Higher eddy diffusivity is related to higher current velocities and since these dominate in spring, it is expected that high eddy diffusion, which is important in the vertical transfer of very fine sediment particles also dominate in spring. Higher eddy diffusivity coefficients also imply a rapid movement of sediments from the channel bottom to the upper section of the water column once a certain critical tidal height and current velocity is reached. This movement is strongly enhanced by eddies generated by currents. The relationship between eddy diffusivity and SSC was strong with correlation coefficient (r) of 0.97 significant at 95% confidence level.

4.8 *Frictional effects and sedimentation in the mangroves*

The net sedimentation in the mangrove swamp in spring was determined along transects running 70 to 450 m from the bank of the main tidal creek to the tidal limit in the mangrove swamp forest near Stn 6. Away from the main tidal channel, there is a decrease in the SSC as one moves inside the mangrove forest. As shown in Fig. 17a, the decrease is rapid with high SSC closer to the main tidal channel (<50 m) than away into the landward limit of the mangrove swamp. Our data shows that SSC in the mangroves is less than 30% of the SSC in the main tidal

channel. The mean SSC along these transects was 0.05 g/l (standard deviation=0.02 g/l). The mean sedimentation rate calculated using the relation W_sC is 0.027 g/m^2/s (±0.01 g/m^2/s) with a maximum of 0.48 g/m^2/s. Time-series data on tidal elevation and SSC inside the mangrove forest showed a rapid decrease in SSC at tidal elevation above 0.30 m. Within a period of 2 h after entry of flood tide water into the mangroves, SSC reduced from 0.16 g/l to less than 0.04 g/l, which is a decline of roughly 70% (Figs. 17b). As seen from Figs. 17b, as the tidal elevation in the mangrove swamp increases during flood tide, SSC reduces rapidly to low values and then declines gently to level out at a concentration range 0.03-0.05 g/l. The decrease is usually more rapid within a period of 1 h after the entry of water in the swamp. During ebb tide the SSC in most cases were much lower, often less than 0.04 g/l (Fig. 17a-b) indicating little re-export of suspended sediments from the mangroves to the main tidal channel. This could partly explain low SSC observed in our data during ebb tide in the main channel. This finding is consistent with that of Furukawa *et al.*, (1997) who have shown that in Middle Creek, Cairns, Australia, SSC is normally higher at flood tide (0.15 g/l) than at ebb tide (0.04 g/l). This indicates net flux of suspended sediment into the mangroves from the tidal channel.

According to Furukawa and Wolanski (1996) and Wolanski *et al.*, (1996), sediment particles settling in the mangrove swamp forest is computed as

$$S_r = W_s C_o \tag{15a}$$

where W_s is the settling velocity and C_o is the initial SSC in the creek channel. The modal SSC (C_o) at the Mwache mangrove swamp is 0.05 g/l with particle settling velocity (W_s) of 0.0005 m/s. Water in the mangrove swamp stays for a period of 3 h per spring tidal cycle. Using these data the sedimentation rate was found to be of the order 250 g/m^2/tide per spring tidal cycle which is comparable to that found by Furukawa and Wolanski (1996) in Australian mangroves (270 g/m^2/tide). However wide spatial variations are expected in light of the differences in the intensity of resuspension, deposition, sediment supply as well as the anthropogenic effects such as mangrove cutting and trampling by humans and animals.

The horizontal variation in SSC in the mangrove swamp has been modelled by Furukawa and Wolanski (1996). Assuming zero-resuspension in the mangrove forest, the equation for conservation of sediment mass can be written as

$$\frac{\partial C}{\partial x} = \frac{-WsC}{hu} \tag{15b}$$

Where C is the SSC, x is the distance across the mangrove forest swamp, h is the water depth and u is the current velocity inside the mangrove swamp. Since the decrease of SSC with distance from the main tidal creek is due to progressive settling out of sediment particles (Furukawa and Wolanski, 1996), the continuity of sediment flux can be expressed as

$$C = C_o.e^{\left(\frac{-W_S x}{hu}\right)} \tag{15c}$$

Where W_s is the sediment settling velocity, C_o is the initial SSC next to the creek main tidal channel and C is the SSC inside the mangrove swamp forest. Equation 15c assumes volume flux into the swamp is not varying. Its aim is to predict and estimate the SSC variation in the mangrove forest given the corresponding parameters in the exponent. Parameters in the exponent ($-W_s x/hu$) vary from one mangrove swamp system to the other and have to be determined for specific cases if the model is to give correct estimates of SSC variations. However, since the volume flux into the swamp, $Q=hu$ is x dependent, complications arise in the prediction of sedimentation patterns in mangroves using the equation 15c.

The SSC computed using Furukawa and Wolanski equation 15c do not compare well with the measured ones (r is 0.63) as is shown in Fig. 22. This is probably due to the fact that Furukawa and Wolanski (1996) assumed that volume flux across a mangrove swamp is uniform which is not realistic since volume flux is a function of time-dependent sea level. In this study, an alternative model that addresses the above problem is proposed. By considering the flow patterns, the total volume flux into the mangrove swamp is written as

$$\frac{dQ}{dy} = -\frac{\partial \eta}{\partial t} = -\eta_t \tag{16a}$$

So that

$$dQ = -\eta_t L \tag{16b}$$

Thus

$$q_o = -\eta_t l \tag{16c}$$

Volume conservation enables determination of horizontal variation of volume flux

$$\frac{dq}{dx} = -\eta_t \tag{16d}$$

Integrating equation 16d using the boundary condition $q=q_o$ when $x=0$ yields

$$q = -\eta_t x + q_o \tag{16e}$$

and introducing Equation 16b into Equation 16e

$$q = -\eta_t (x - l)$$

(16f)

The conservation of suspended sediment then is written as follows

$$\frac{1}{C}\frac{\partial C}{\partial x} = -\frac{W_s}{q} = \frac{W_s}{\eta_t}\frac{1}{x-l} = -\frac{W_s}{\eta_t}\frac{1}{l-x}$$

(16g)

Hence

$$\ln C = \frac{W_s}{\eta_t}\ln(l-x) + A$$

(16h)

Thus SSC variation in the mangrove forest swamp can be modeled as

$$C = A*(l-x)^{\frac{W_s}{\eta_t}} = C_o\left[\frac{l-x}{l}\right]^{\frac{W_s}{\eta_t}}$$

(16i)

since $C = C_o$ when $x = 0$. In Equation 16i, C_o is the initial SSC at the mangrove forest edge adjacent the main tidal channel, C is the SSC at distance x, l is the total length of the mangrove swamp, W_s is the sediment particle settling velocity and η_t is the sea level change with time. Equation 16i is a stationary one and so is only applicable if the sedimentation time-scale is longer than the tidal time-scale. The comparison of SSC computed using the Equation 16i and measured ones shows the prediction is not perfect but is good enough with r value of 0.66 (Fig 22). This lack of perfect prediction may due to the fact that bottom topography is not considered as one of the parameters in the equation 16i. This causes the divergent of the predicted SSC from the measured SSC as distance from the channel bank increases.

Measurements of flow velocities shows that velocities within the Mwache mangrove swamp are weak, often less than 0.10 m/s. This is attributed to frictional effects of dense mangrove roots as reported also in Australian mangrove creeks (Furukawa *et al.*, 1997). Thus suspended sediments brought into the mangrove forest in flood tide settles rapidly in the swamp (Fig. 17a-b) because low flow velocities do not cause high turbulence which is an important prerequisite for keeping sediment particles in suspension. Most of the incoming sediments settles out in the mangrove swamp and there is limited re-export as is evidenced by relatively low SSC during ebb tide.

4.9 *Accretion in the mangrove swamp forest*

The term accretion (A_r) different from the deposition rate (S_r) as used in this study refers to the rate at which suspended sediments accumulate. In case of Mwache creek, was calculated as

$$A_r = \frac{S_r}{B_\rho} \tag{17}$$

where B_ρ, the sediment bulk density is the ratio between the weight of sediments and their corresponding volume. Gross sedimentation rates (S_r) were calculated using Equation 15a. The sediment bulk density for Mwache creek sediments was found to be of the order 1800 Kg/m^3. If the typical gross sedimentation rate of 250 g/m^2 per spring tide is applied in equation 17, an accretion rate of roughly 30 cm/100 years is obtained for Mwache creek mangrove swamp. This is comparable to accretion rates reported by other workers in similar mangrove systems in the Caribbean, Malaysia and Australia (Ellison, 1993; Furukawa *et al.*, 1997 and Saad *et a.l*, 1999). For example, Ellison (1993) found the sediment accretion rates in Bermuda to be of the order 8.5 to 10.6 cm/100 years which are lower than the local sea-level rise of 28 cm±18 cm/100 years. Furukawa *et al.*, (1997) found the accretion rate to be 10 cm/100 years in the Middle Creek, Cairns, Australia. In a recent study, Saad *et al.*, (1999) reported accretion rate in Malaysian estuarine mangrove swamps to be 146 cm/100 years, which is much higher than the local sea level rise of 0.1-0.5 cm/yr. In Brazilian mangroves, Smoak and Patchineelan (1999) reported sediment accretion rates in the order of 12-18 cm/100 years which is also higher than the estimated local sea level rise of 1 cm/year.

5. DISCUSSIONS

In the 1998-1999 period during which this study was conducted, both short and long rains were below average and there was no major river runoff. However in 1997, particularly in the period between October and November, heavy rainfall associated with the *El Nino* caused tremendous increase in river discharge of both freshwater and terrigenous sediments. In normal years, seasonal rivers draining into Mwache creek flow for about 120 days. During rainy season, river SSC is usually in the order 0.5 g/l, but is relatively much lower in drier periods. This with the average river discharge of 10 m^3/s indicates that, rivers supply an equivalent of 5 x 10^4 tons of terrigenous sediments into the creek on annual basis (Table 1). This is roughly suspended sediment flux of about 7 Kg/s, which is of the same order of magnitude as the sediment deposition rate in the mangroves of the order 250 g/m^2/spring tide. This shows that most of the sediments brought in by the rivers are trapped within the creek and constantly reworked by the tidal currents.

SSC is usually higher in flood tide as compared to ebb tide (Fig.14a-b). The high SSC at spring flood in the creek could be due to erosion of the channel bed as well as to the remobilization of sediments deposited during the *El Nino* and monsoon rainfall events. Both maximum and minimum SSC occurs during spring. However, at high tide during periods of accelerating currents, sediments are advected from the bottom to the surface water column due

to strong currents (Figs. 13 and 14a-b). The relationship between SSC and current velocities shows significant increase in SSC occurs with increasing current velocities (Figs. 20-21). Similar results have been reported by Schoelhamer (1995) and Furukawa *et al.*, (1997). Re-suspension dominate during flood tide despite the fact that ebb tide current velocities are as high as those in flood tide. Lack of resuspension in ebb tide and major resuspension in flood tide explains a large net flux of suspended sediments into the creek (Fig. 16). This however was unexpected in view of a slight dominance of ebb current velocities although the asymmetry in both sea level and current velocities is not so well developed to favour a net flux out of the creek. Although high SSC occur during spring near-high water, there was a tendency for relatively much lower SSC to occur in spring low water and relatively higher mean concentrations during neap low water (Figs.14a-b). This rather interesting observation could at the first glance be attributed to the clogging on the OBS sensor, but an alternative explanation can also be sought. This is attempted by considering the differences in the respective spring and neap variation of tidal elevation and range. During spring, the large tidal range is well above 3.0 m implying that low tide water depth is much lower than in neap, so that at low tide, the mean depth is roughly 3 m (Table 5). With the suspended sediment settling velocity of the order 0.0005 m/s, suspended sediments in the 3-4 m water column depth could settle almost completely within a period of 2 h when current velocities are low. However during neap, the tidal range is small approximately 1.4 m and therefore the mean low water depth is higher being about 6 m, hence suspended sediments do not settle out completely within 2 h during slack waters before the turn of the tide.

The resuspension-deposition patterns can also be related to the neap-spring differences in the thickness of the water column. Currents at the beginning of flood tide can transmit turbulence down the channel bottom much more rapidly in a water column of limited extent than a large one. Thus more rapid rises in SSC during flood tide occurs in spring as compared to neap. Also small waves in shallow waters during spring low can disturb the bottom sediments thus leading to higher SSC since wave energy is rapidly transmitted down to the water column of limited depth extent.

Calculation of erosion and deposition rates according to Equations 9b and 9d shows that erosion in the creek is much larger than the deposition (Figs.18a-b). The erosion rates reach as high as 6×10^{-4} Kg/m^2/s while deposition rates reach 5.0×10^{-5} Kg/m^2/s. This implies that SSC production usually available for transport is of the order 5×10^{-4} Kg/m^2/s. Although these results are reasonably well within the acceptable limits of erosion and deposition, large spatial-temporary anomalies are likely to result since they are dependent on subjective judgement on the critical velocities for erosion and deposition. The critical velocities are expected to be spatially variable (Figs. 20-21). This spatial variability may be more pronounced where the sediments of different particle sizes occur in different locations of the creek. Our computed rates of erosion and deposition are within the range reported in other studies. For example, Amos *et al.*, (1992 and 1997) found for subaerially exposed muds, sediment erosion rate vary from 1.0×10^{-4} to 7.5×10^{-4} Kg/m^2/s (cf. Widdows *et al.*, 1998 and Houwing, 1999). Higher rates of channel erosion as compared to deposition imply that tidal channels fringing mangroves do not silt up and therefore remain free of sediments in most periods of the year. With a mangrove area of 12 Km^2 and typical sedimentation rate of 250 g/m^2/spring tide, it is estimated that the total quantity of sediments deposited in the mangrove swamp in one spring tide may reach as high as 3000 tonnes. Large inflow of sediments into the mangrove swamp may impact

negatively on them since mangroves are severely stressed when their breathing roots are covered with fine-grained sediments.

The spatial variation of current velocities in creek may partly explain the formation of a turbidity maximum zone (TMZ) in the upper zones (Stns 3-6) fringing the mangrove swamp. The TMZ is more developed in spring than in neap tide, because of stronger currents during spring than during neap, a finding which is consistent with that of Wolanski *et al.*, (1998). The occurrence of high salinity in the region of high SSC, allows us to suspect that there could be a relationship between salinity maximum zone (SMZ) and TMZ. The sinking of dense highly saline surface water probably generates vertical convective eddies which induces vertical sediment flux and thus causes localized increase in SSC in the TMZ. The SMZ characterised by the presence of relatively high salinity water is formed as result of accelerated evaporation in shallow waters (cf. Hoguane *et al.*, 1999). This phenomena has never been reported previously in the mangrove wetlands of East Africa, but there have been several reports about it in systems which are different from Mwache creek (Wolanski *et al* 1995; Uncles *et al.*, 1994; Geyer, 1993 and Wellershaus, 1981).

It seems certain that processes influencing the generation of TMZ in the Mwache creek are different from those in salt-wedge estuaries as reported in Geyer (1993) and Wellershaus (1981). In such estuaries, the convergence of dense oceanic water flowing beneath the less dense river water leads to entrainment of the bottom sediments at the tip of the salt-wedge into interface. This increases SSC in the lower reach of salt-wedge estuaries as reported by Wolanski *et al.*, (1995) and Uncles *et al.*, (1994). In our case, it seems that TMZ is due to the existence of certain zones within the main channel where tidal pumping causes currents of much stronger velocities of the order 1 m/s which are capable of resuspending bottom sediments (Fig. 18a-d). The influence of the channel morphology and bathymetry is therefore important in case of Mwache creek.

While there is a tidal current velocities asymmetry characterized by somewhat stronger ebb than flood current velocities (Fig.5a-b, 7a-b), there is hardly any major asymmetry in tidal elevations (Fig.5b). The ebb and flood tide are more or less similar. From our data it seems that the existence of current asymmetry does not favor a net seaward transport of sediments as reported by Wolanski *et al.*, (1980), but is consistent with the findings of Gao *et al.*, (1990). This point arises due to the fact that, the results of observation of sediment fluxes show flood dominance although the ebb velocities are slightly higher than flood ones (Fig. 15). This however is explained when one considers the simultaneous observations of SSC and current velocities which shows that far much greater re-suspension of bottom sediments occur during flood tide (Fig. 14a-b).

It is possible that wind-waves in the Kipevu basin also resuspends bottom sediments during low waters so that when flood tide begins there is advection of water with high SSC into the Mwache creek (Fig. 13). However in the narrow tidal channels, particularly those beyond station 6, elevated tidal current velocities are necessary in maintaining high SSC levels away from the area of resuspension.

Although neap-spring cycle in SSC could not be demonstrated perfectly due to improper setting of the SSC threshold in OBS sensor, it is still possible to discern a significant difference between neap and spring SSC in our data (Fig. 14a-b). Periods of maximum SSC in spring (flood tide) are short-lived and appear only during a few hours during high water spring (HWS) as shown in Fig.14a-b (cf. Wolanski *et al.*, 1995 and Wolanski *et al.*, 1998). Greater resuspension occurs during spring tide and it is therefore expected that this is the time during

which large quantities of sediments are removed from the tidal channels and deposited in the mangrove swamp. Suspended sediments entering the mangrove swamp are effectively trapped there since the dense network of mangrove trunks and pneumatophores result in low current velocities. Flows in the mangrove swamp are sluggish and cannot keep sediments in suspension for long time and results in deposition of sediments within an hour of entry in the mangrove swamp (Fig. 17b) as was similarly demonstrated by Furukawa *et al.*, (1997) and Furukawa and Wolanski (1996). There is very little re-export of the suspended sediments from the mangrove swamp during ebb flow and probably this explains low SSC observed during ebb tide at the main channel. Sediments deposited west of Kipevu basin are partially exposed during spring low tide and are inadvertedly sources of sediments that are pumped back into the mangrove wetland during spring flood tide. This seems to be so in dry periods of very low river sediment supply, when the wetland is supposedly under-nourished with terrigenous sediments and the only source of sediments is tidal channels and material deposited in the previous rainy season at Kipevu basin.

In East Africa, sea level is estimated to be rising at a rate of 22 cm/100 years (IOC-UNESCO, 1994 and Lennon, 1994) which is lower than the rate at which the Mwache mangrove sediments are building up. This finding is consistent with the similar findings in estuarine mangrove forests in Malaysia (Saad *et al.*, 1999). Examination of the aerial photographs of the Port-Reitz creek area taken in the 1970s as well as the present bathymetric charts, in addition to surveys by the author, shows evidence of accelerated rates of tidal channel erosion and sediment deposition in Kipevu basin. The main tidal channel in the creek is much wider than it used to be in 1970s and a large sediment deposition feature West of shallow Kipevu basin (absent in 1970s aerial photograph), is now a prominent geomorphological feature which is presently being colonized by the mangroves. Local sea level rise associated with global warming is expected to reach 65 cm±35 cm by the end of the next century (IOC-UNESCO, 1994; Lennon, 1994). It is likely that there would be even more accelerated channel erosion in tidal creeks and heavy deposition in mangroves and in the shallow Kipevu basin.

6. CONCLUSIONS

This study focussed on the tidal dynamics, SSC variations and sediment fluxes in the Mwache mangrove creek during periods of relatively low river discharge. It was found that zones located in the lower region (Stns 7-8) fronting the open Indian Ocean are characterized by low SSC in the range 0.01-0.08 g/l. The upper mangrove zone (Stns 1-6) is characterized by high SSC in the range 0.02-1.40 g/l. The bottom SSC in the upper zones of the creek was mainly of the order 1.40 g/l, but was of the order 0.10 g/l in the frontwater zone. The observed SSC variations are primarily due to semi-diurnal tides and varying current velocities, which control re-suspension and transport processes into and out of the creek. High re-suspension and transport dominates in spring and deposition in neap so that high SSC occur in spring and lower ones in neap. The mean suspended sediment fluxes in spring and neap are 1215 and 400 Kg/s respectively. The sediment fluxes are usually higher during flood tide (460-1740 Kg/s) than during ebb tide (340-690 Kg/s) in both spring and neap. SSC increases as flood current velocities increase but this is not true during ebb tide. Resuspension of bottom sediments dominates when maximum flood current velocities of the order 1 m/s occur during spring.

Since most of the sediments resuspended during flood tide enter the mangroves where they are trapped, SSC during ebb tide are usually low even at high ebb current velocities.

A turbidity maximum zone (TMZ) characterized by relatively higher SSC in the range 0.10-0.16 g/l occurs between Stn 3 and 6. In the dry season when the creek receives little sediments from the rivers, sediments are imported into the creek from the Kipevu basin. In addition to sediments imported from Kipevu basin, sediments eroded from the main tidal channels are partly exported into the mangrove swamp forest and this in the long run ensures that the tidal channels do not fill up with sediments. Also the influx of suspended sediments into the mangroves help to build the mangrove forest sediments thus keeping up in pace with sea level rise. The accretion rate in the mangroves was estimated to be of the order 30 cm/100 years, which is higher than the estimated local sea level rise of 22 cm/100 years. Trapping of sediments in the mangroves is due to dense mangrove vegetation and gentle slope that results in low flow velocities, less than 0.10 m/s. These low velocities cannot keep sediments in suspension for long time and so there is rapid settling of sediments. Whether the mangrove acreage will decrease or increase in light of the processes discussed in this thesis, is still a subject of motivated debate and the effects of increased river discharge and sea level rise on the overall sustainability of the mangroves remain to be determined conclusively. Due to prevalence of drought, it was not possible to establish the conditions in rainy seasons when the supply of river sediments and freshwater is high. This research should however set the basis for more studies aimed at establishing the connection between hydrodynamics, sediment transport and sustainability of mangrove creek forests. This is partly in view of the immense socio-economic and environmental value of the mangrove wetlands.

REFERENCES

Aldridge, J.N. (1997): Hydrodynamic model predictions of tidal asymmetry and observed sediment transport paths in Morecambe Bay. *Estuarine, Coastal and Shelf Science* 44: 39-56.

Althausen, J.D and Kjerfve, B. (1992): Distribution of suspended sediment in a partially mixed estuary, Charleston Harbor, South Carolina, USA. *Estuarine, Coastal and Shelf Science* 35: 517-531.

Amos, C.L., Darbon, G.R and Christian, H.A. (1992): *In situ* erosion measurements on fine-grained sediments from the Bay of Fundy. *Marine Geology* 108: 175-196.

Amos, C.L., Feeney, T., Sutherland, T.F. and Luternauer, J.L. (1997): The stability of fine-grained Sediments from the Fraser River Delta. *Estuarine, Coastal and Shelf Science* 45: 507-524.

Ayukai, T and Wolanski, E. (1997): Importance of Biologically Mediated Removal of Fine Sediments from the Fly River plume, Papua New Guinea. *Estuarine, Coastal and Shelf Science* 44: 629-639.

Caswell, P.V. (1956): Geology of Kilifi - Mazeras areas. *Government Printer*, Nairobi, Kenya, 41p.

Cederlof, U. (1998): Short lecture notes for MSc course in Physical Oceanography. Part I: *Geophysical fluid dynamics*. Gothenburg University, Sweden, 8-9.

Cederlof, U., Rodhe, J., Rydberg, L and, Sehlstedt, P. (1996): Technical note: performance study of the Haamer gelatin pendulum current meter. *Journal of Sea Research* 35(1-3): 55-61.

Daily Nation (30 May, 1999): Crab, Prawn farming hold hope for Tsunza. p. IV.

Dyer, K.R.(1979): Estuarine hydrography and sedimentation. *Cambridge University Press*, London, 230p.

Ellison, J.C. (1993): Mangrove retreat with rising sea level, Bermuda. *Estuarine, Coastal Shelf Science* 37: 75-87.

Furukawa, K and Wolanski, E. (1996): Sedimentation in mangroves forests. *Mangroves and Salt Marshes* 1(1): 3-30.

Furukawa, K; Wolanski, E and Mueller, H. (1997): Currents and sediment transport in mangrove forest. *Estuarine, Coastal and Shelf Science* 44: 301-310.

Gao, S and Colins, H. (1990): Tidal inlet equilibrium in relation to cross-sectional area and sediment transport patterns. *Estuarine, Coastal and Shelf Science* 38: 157-172.

Gao, S., Xie, Q.C and Feng, Y.J. (1990): Fine-grained sediment transport and sorting by tidal exchange in Xiangshan Bay, Zhejiang, China. *Estuarine, Coastal and Shelf Science* 31: 397-409.

Geyer, W.R (1993): The importance of suppression of turbulence by stratification on the estuarine turbidity maximum. *Estuaries* 16 (1): 113-125.

GOK (1975): Mombasa water pollution and waste disposal: marine investigations, Part VI. *NORCONSULT A.S Report*, Nairobi, Kenya. 5.11-5.20.

Grosskopf, P.E and Onyango, V.O. (1991): Numerical analysis of sedimentation in the expanded channel, Mombasa Port at Dongo Kundu, Kenya. *In the Proceedings of the Third International Conference on Coastal and Port Engineering in Developing countries*, Mombasa, Kenya, 16th-20th September 1991.Vol. II. 1925-1936.

Hoguane, A.M., A.E. Hill., J.H Simpson and Bowers, D.G. (1999): Diurnal and tidal variation of temperature and salinity in the Ponta Rassa Mangrove Swamp, Mozambique. *Estuarine, Coastal and Shelf Science* 49: 251-264.

Houwing, E.J. (1999): Determination of the critical erosion threshold of cohesive sediments on intertidal mudflats along the Dutch Wadden sea coast. *Estuarine, Coastal and Shelf Science* 49: 545-555.

IOC-UNESCO (1994): IOC-UNEP-WMO-SAREC Planning Workshop on an Integrated Approach to Coastal Erosion, Sea-Level changes and their impacts. Zanzibar, 17-21, Jan. 1994. *IOC-UNESCO Workshop report No. 96, supplement 2*, 104p.

Kitheka, J.U. (1996): The dynamics of Mwache river basin sediment production and discharge and, flux of terrigenous sediments in Port-Reitz Creek, Kenya. *WIOMSA /IOC Project* (SC 298-012-5) Report, 68p.

Lennon, G.W. (1994): Sea-level variation and changes in the Indian Ocean. *IOC Workshop Report no. 96, Supplement 2*, 17-19.

Leonard, L.A., Hine, A.C., Luther M.E., Stumpf, R.P and Wright, E.E. (1995): Sediment transport processes in a West-Central Florida Open Marine Marsh Tidal Creeks: the role of tides and extra tropical storms. *Estuarine, Coastal and Shelf Science* 41: 225 - 248.

Lindsay, P., Balls, P.W and West, J.R. (1996): Influence of tidal range and river discharge on suspended particulate matter fluxes in the North Estuary (Scotland). *Estuarine, Coastal and Shelf Science* 42: 63-82.

Lund-Hansen, L.C., Pejrup, M., Valeur, J and Jansen, A. (1994): Eddy diffusion coefficients of suspended particulate matter: effects of wind energy transfer and stratification. *Estuarine, Coastal and Shelf Science* 30: 559-568.

Mazda, Y., Kanazawa, N. and Wolanski, E. (1995): Tidal asymmetry in mangrove creeks. *Hydrobiologia* 295: 51-58.

Magori, C (1999): Unpublished tide prediction tables for Mombasa: hourly predictions. *KMFRI,* Mombasa, Kenya. 13p.

Manning, A.J and Dyer, K.R. (1999): A laboratory examination of floc characteristics with regard to turbulent shearing. *Marine Geology* 160 (1-2): 147-170.

McGave, I.N (1979): Suspended sediment. In: Dyer, K.R (1979): Estuarine hydrography and sedimentation. *Cambridge University Press*, London, 230p.

Prindle, D., Hydes. D., J. Jarvis and McManus, J. (1997): The seasonal cycles of temperature, salinity, nutrients and sediment in the Southern North Sea in 1988 and 1989. *Estuarine, Coastal and Shelf Science* 45: 669 - 680.

Poulos, S.E and Collins, M.B. (1994): Effluent diffusion and sediment dispersion at Micro-tidal river mouths predicted using mathematical models. *Estuarine, Coastal and Shelf Science* 38: 189-206.

Rade, L and Westergren, B. (1990): BETA- Mathematics Handbook, 2nd Edition. *Chartwell-Bratt*, 494p.

Saad, S., Husain, M.L., Yaacob, R and Asano, T. (1999): Sediment accretion and variability of sedimentological characteristics of a tropical estuarine mangrove: Kemaman, Terengganu, Malaysia. *Mangroves and Salt Marshes* 3: 51-58.

Schoelhamer D.H. (1995): Sediment re-suspension mechanisms in Old Tampa Bay, Florida. *Estuarine, Coastal and Shelf Science* 40: 603-620.

Smoak, J.M and Patchineelam, S.R. (1999): Sediment mixing and accumulation in a mangrove ecosystem: evidence from ^{210}Pb, ^{234}Th and ^{7}Be. *Mangroves and Salt Marshes* 3: 17-27.

Steel, R.G.D and Torrie, J.H. (1991): Principles and procedures of statistics; a biomedical approach, 2nd edition. *McGraw-Hill Book Company*, London, 633p.

Uncles, R.J., Barton, M.L and Stephens, J.A. (1994): Seasonal variability of fine sediment concentrations in the turbidity maximum region of the Tamar estuary. *Estuarine, Coastal and Shelf Science* 38: 19-39.

Uncles, R.J; Elliot, R.C and Weston, S.A. (1985): Observed fluxes of water, salt and suspended sediment in a partially mixed estuary. *Estuarine, Coastal and Shelf Science* 20: 147-1687.

Vogel, R.L., Kjerfve, B and Gardner, R.L. (1996): Inorganic sediment budget for the North inlet Salt Marsh, South Carolina. *Mangroves and Salt Marshes* 1(1): 23-35.

Wellerhaus, S. (1981): Turbidity maximum and mud shoaling in the Weser estuary. *Arch. Hydrobiol.* 92(2): 161-198.

Widdows, J., Brinsley, M.D., Bowley, N and Barrett, C. (1998): A benthic annular flume for *in situ* measurements of suspension feeding/biodeposition rates and erosion potential of cohesive sediments. *Estuarine, Coastal and Shelf Science* 46: 27-38.

Wolanski, E., Huan, N.N., Dao, L.T., Nhan, N.H and Thuy, N.N. (1996): Fine sediment dynamics in the Mekong River estuary, Vietnam. *Estuarine, Coastal and Shelf Science* Vol. 43, 565-582.

Wolanski, E., Jones, M and Bunt, J.S. (1980): Hydrodynamics of a tidal creek mangrove swamp systems. *Australian Journal of Marine and Freshwater Research* 13: 431-450.

Wolanski, E., King, B and Galloway, D. (1995): Dynamics of the turbidity maximum in the Fly River estuary, Papua New Guinea. *Estuarine, Coastal and Shelf Science* 40: 321-337.

Wolanski, E., Gibbs, R.J., Spagnol, S., King, B and Brunskill, G. (1998): Inorganic sediment budget in the mangrove-fringed Fly River Delta, Papua New Guinea. *Mangroves and Salt Marshes* 2: 85-98.

Wolanski, E., Nhan N.H and Spagnol, S. (1998): Sediment dynamics during low flow conditions in the Mekong River estuary, Vietnam. *Journal of Coastal Research* 14(2): 472-482.

List of symbols

τ	Shear stress.
τ_c	Bottom shear stress.
ρ	Seawater density.
κ	von Karman's constant.
η_t	Sea level change with time ($\partial\eta/\partial t$).
η	Free surface height.
A	Coefficient in harmonic analysis.
A_c	Cross-sectional area.
A_N	Creek's surface area as a function of depth.
A_j	Surface area covered at specific water depth.
A_o	Creek's surface area at mean sea level.
A_r	Accretion rate in the mangrove swamp forest.
A_s	Creek's total surface area.
A_z	Eddy diffusivity.
B	Coefficient in harmonic analysis.
B_ρ	Bulk density of the sediment.
C	Depth integrated suspended sediment concentration.
C_d	Drag coefficient.
C_o	Initial suspended sediment concentration within the tidal channel.
F	Coefficient in harmonic analysis.
F_o	Sediment deposition rate at the mangrove zone next closer to the tidal channel.
GS	Gross sedimentation rate in the mangrove swamp forest.
H	Water depth.
h_j	Specific water depth.
k	Frequency.
K	Length of the sea level record.
L	Total length of the mangrove swamp.
M_d	A term representing sediment deposition in the tidal channel bed.
M_e	A term presenting sediment erosion in the tidal channel bed.
N	Sample size.
Q	Tidal volume flux in the main channel along the horizontal axis.
q	Volume flux into the mangrove swamp forest.
Q_e	Ebb tide volume flux in the main channel.
Q_f	Flood tide volume flux in the main channel.
Q_{np}	Tidal volume flux in the main channel during neap.
q_o	Total volume flux into the mangrove swamp forest.
Q_s	Suspended sediment flux in the main tidal channel.
Q_{sp}	Tidal volume flux in the main tidal channel during spring.
r	Correlation coefficient.
R^2	Coefficient of determination.
R_e	Tidal range during neap.
R_f	Tidal range during spring.
s	Standard deviation.

S_r	Sediment deposition rate.
t	Time period or duration.
T_e	Duration of ebb tide.
T_f	Duration of flood tide.
U	Current velocity within the main tidal channel.
u	Flow velocity in the mangrove forest swamp.
U_*	Friction velocity.
U_d	Critical velocity for sediment deposition.
U_e	Critical velocity for sediment erosion.
U_{eb}	Mean ebb tide velocity in the main channel.
U_f	Mean flood tide velocity in the main channel.
U_x	Mean current velocity.
U_z	Current velocity in the boundary layer.
ΔV_s	Spring tidal prism.
ΔV_n	Neap tidal prism.
ΔV_T	Tidal prism at mean sea level.
V	Total water volume.
V_N	Volume at specific water level.
V_e	Low water volume.
V_h	High water volume.
W_s	Sediment settling velocity.
x	Horizontal distance.
X	Coordinate distance.
z	Vertical distance or vertical extent of the water column.
Z	Sea level record.
Z_*	Boundary or friction layer.
Z_o	Channel bed roughness length.

Table 1: The areal extent of mangrove swamps and tidal creeks in Port-Reitz mangrove wetland. The areas were determined from the 1:50,000 topographic map.

Basin	Mangroves (Km^2)	Tidal creeks (Km^2)	Total Area (Km^2)
1. Mwache	11.97	4.80	16.97
2. Mteza	9.36	3.11	12.47

Table 2: The drainage basins, river discharges and sediment supply to Port-Reitz creek. Mwache and Mambome seasonal rivers discharge directly into Mwache creek.

Basin	Area (Km^2)	Discharge (m^3/s)	Sediment supply (Kg/s)	Sediment Discharge (Tons/yr.)
1. Mwache	1703	8.64	4.30	$4.46x10^4$
2. Cha-Simba	614	3.12	1.60	$1.16x10^4$
3. Mambome	212	1.07	0.50	$0.50x10^4$
4. Manjera	98	0.50	0.25	$0.26x10^4$
TOTAL				**$6.88x10^4$**

Source: Kitheka, 1996.

Table 3: Standard table for classification of tides based on the F-ratio scale.
The F-ratio for Port-Reitz creek is 0.188 representing purely semi-diurnal tide.

Form number (F) $(F=(K_1 + O_1)/(M_2 + S_2)$	**Type of tide**
$0<F<0.25$	Purely semi-diurnal
$0.25<F<1.5$	Mixed, mainly semi-diurnal
$1.5<F<3.0$	Mixed, mainly diurnal
$F>3.0$	Purely diurnal

Table 4: The results of harmonic analysis of sea-level record at Stn 6 based on 22 days measurements in February, 1999. Amplitudes less than 0.015 m could be discarded since they are lower than the resolution of the MicroTide pressure gauge used in the measurement.

Tidal Constituent	**Period (hrs)**	**Amplitude (m)**
Diurnal		
O_1	25.82	0.09
P_1	24.07	0.02
K_1	23.93	0.20
Semi-Diurnal		
N_2	12.66	0.17
M_2	12.42	1.10
S_2	12.00	0.44
K_2	11.97	0.18
Shallow water		
M_4	6.21	0.02
M_6	4.14	0.01
S_4	6.00	0.01
Others		
$2SM_2$	11.61	0.02
MS_4	6.10	0.02
$2MS_6$	4.09	0.02
M_f	327.87	0.04

Table 5: Spring and neap semi-diurnal tidal ranges based on main tidal constituents. Spring tide lag from the local passage of new or full moon is computed as $0.98(S_2 - M_2)$. High tidal range in spring tide is associated with high tidal prism.

Spring	2.0 ($M_2 + S_2$)	3.1 m
Neap	2.0($M_2 - S_2$)	1.3m
Mean	2.2 M_2	2.4m

Table 6: The mean spring and neap tidal current velocities and tidal volume flux in the period Feb. 2-23, 1999 and suspended flux in the period Feb. 15-23, 1999. These are based on time series measurements at Stn 6.

	Spring tide	Neap Tide
Mean flood tidal volume flux (m^3/s)	2179	914
Mean ebb tidal volume flux (m^3/s)	2286	959
Mean flood velocity (m/s)	1.25	0.52
Mean ebb velocity (m/s)	1.30	0.55
Mean flood sediment flux (Kg/s)	1740	460
Mean ebb sediment flux (Kg/s)	690	340

Table 7: The summary statistics (based on monthly surveys) for variables measured at Port-Reitz Creek in the period between March 1998 and March 1999. SSC, SAL and TEMP in the table refer to suspended sediment concentration, salinity and temperature respectively. Corresponding numbers refers to sampling stations. Stns 1, 6 and 10 are in the upper, middle and lower regions of the creek respectively.

Variable	Valid N	Mean	Minimum	Maximum	Std. Dev.
SSC-1 (g/l)	11	0.163	0.019	0.900	0.278
SSC-6 (g/l)	12	0.033	0.011	0.080	0.021
SSC-10 (g/l)	12	0.029	0.011	0.073	0.020
SAL-1	11	23.59	1.51	36.40	12.28
SAL-6	11	34.21	29.44	36.22	2.30
SAL-10	11	34.74	30.98	35.82	1.55
TEMP-1 (c)	11	29.10	25.88	31.19	1.60
TEMP-6 (c)	11	28.25	24.63	31.50	2.12
TEMP-10 (c)	11	28.20	24.58	31.60	2.26

Table 8: Summary data based on several 12-25 h time-series measurements conducted twice a month at Stn 6 in the period between March 1998 and March 1999. SSC, Sal and temp stands for suspended sediment concentration, salinity and temperature. Surf-, Mid- and Bott- refers to the source of the sample, whether surface, middle or bottom water column.

Variable	Valid N	Mean	Minimum	Maximum	Std. Dev.
Current (m/s)	69	0.30	0.0	0.93	0.21
SurfSSC (g/l)	69	0.052	0.026	0.151	0.033
MidSSC (g/l)	35	0.038	0.0287	0.071	0.0084
BottSSC (g/l)	69	0.060	0.026	0.197	0.036
SurfSal	38	35.96	32.06	37.69	1.64
MidSal	38	36.03	32.84	37.42	1.39
BottSal	38	36.06	33.40	37.34	1.27
Surftemp ©	48	27.76	25.68	30.36	1.20
Midtemp ©	38	27.95	25.53	30.36	1.25
Bottemp ©	48	27.79	25.53	30.00	1.10
Sechii (m)	48	0.99	0.40	2.40	0.53

Table 9: The descriptive statistics for variables measured on monthly basis at Stn 6 in the period between March 1998 and March 1999. Data includes combined results for measurements conducted in both neap and spring periods.

Variable	Valid N	Mean	Minimum	Maximum	Std. Dev.
Surftemp ©	8	27.86	24.22	30.29	1.96
Midtemp ©	7	27.49	23.92	31.15	2.24
Bottemp ©	7	27.47	23.67	31.54	2.46
SurfSal	7	33.92	27.81	37.60	3.76
MidSal	6	33.91	27.71	37.33	3.81
BottSal	6	34.02	27.71	37.24	3.74
SurfSSC (g/l)	9	0.04	0.01	0.11	0.03
MidSSC (g/l)	9	0.07	0.02	0.20	0.067
BottSSC(g/l)	9	0.13	0.03	0.70	0.217
Sechii (m)	8	1.16	0.70	2.20	0.469

Table 10: The descriptive statistics for variables measured on monthly basis at Stn 1in the precincts of the Mwache estuary (March 1998-March 1999). Note large standard deviation for salinity and temperature in the estuary.

Variable	Valid N	Mean	Minimum	Maximum	Std. Dev.
SurfTemp ©	9	29.68	25.88	33.0	2.45
Midtemp ©	8	29.41	25.53	32.70	2.45
Bottemp ©	8	29.31	24.98	32.50	2.62
SurfSal	8	19.47	1.51	36.04	12.02
MidSal	7	20.02	1.37	36.00	11.57
BottSal	7	22.07	7.83	36.00	9.52
SurfSSC (g/l)	10	0.22	0.02	1.45	0.44
MidSSC (g/l)	10	0.19	0.02	0.91	0.27
BottSSC (g/l)	10	0.44	0.03	1.39	0.55
Sechii (m)	8	0.53	0.30	1.00	0.26

Table 11. Descriptive statistics for variables measured on monthly basis at Stn 9 near Kipevu (March 1998-March 1999). Note the relatively narrow salinity range at the station as compared to the inner stations fringing the mangroves.

Variable	Valid N	Mean	Minimum	Maximum	Std. Dev.
Surftemp ©	8	28.32	24.63	32.00	2.28
Midtemp ©	8	28.24	24.53	31.80	2.26
Bottemp ©	8	28.14	24.78	31.60	2.18
SurfSal (m)	7	33.35	29.44	35.91	2.47
MidSal (m)	7	34.13	31.67	36.00	1.49
BottSal (m)	7	34.33	31.06	36.30	1.65
SurfSSC (g/l)	10	0.03	0.01	0.06	0.013
MidSSC (g/l)	10	0.02	0.01	0.05	0.010
BottSSC (g/l)	10	0.05	0.02	0.11	0.031
Sechii (m)	10	1.58	0.60	3.00	0.75

Table 12: The descriptive statistics for variables measured on monthly basis at Stn 10 near Likoni Ferry in the period between March 1998-March 1999. The station is located at the narrow entrance which connects the Port-Reitz creek (Kilindini channel) with the Indian Ocean.

Variable	Valid N	Mean	Minimum	Maximum	Std. Dev.
Surftemp ©	7	28.31	25.28	31.00	2.32
Midtemp ©	6	28.09	25.33	30.60	2.28
Bottemp ©	6	28.07	25.10	30.50	2.24
SurfSal	6	34.17	30.98	35.82	1.93
MidSal	5	33.62	30.94	35.78	2.27
BottSal	5	34.30	31.24	35.80	1.83
SurfSSC (g/l)	9	0.033	0.01	0.117	0.034
MidSSC (g/l)	9	0.025	0.011	0.058	0.014
BottSSC (g/l)	9	0.032	0.016	0.063	0.016
Sechii (m)	9	2.68	1.00	5.000	1.5

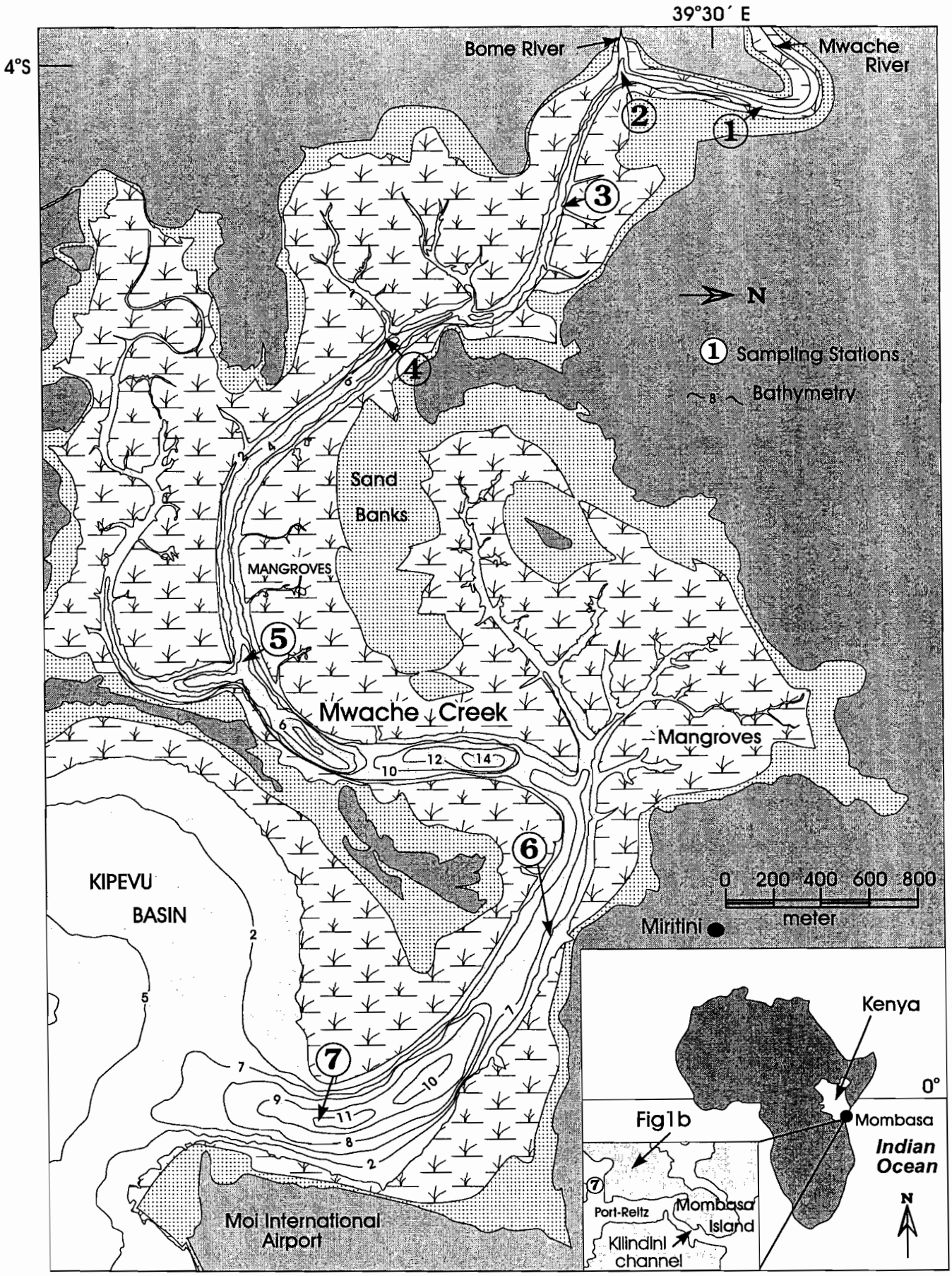

MWACHE CREEK

Fig. 1: Map of Mwache Creek with the locations of sampling stations. The principal stations are Stns 1, 4, 6 and 8. For surface area and volume computations, the whole mangrove extent and associated tidal creeks above Stn 7 were considered.

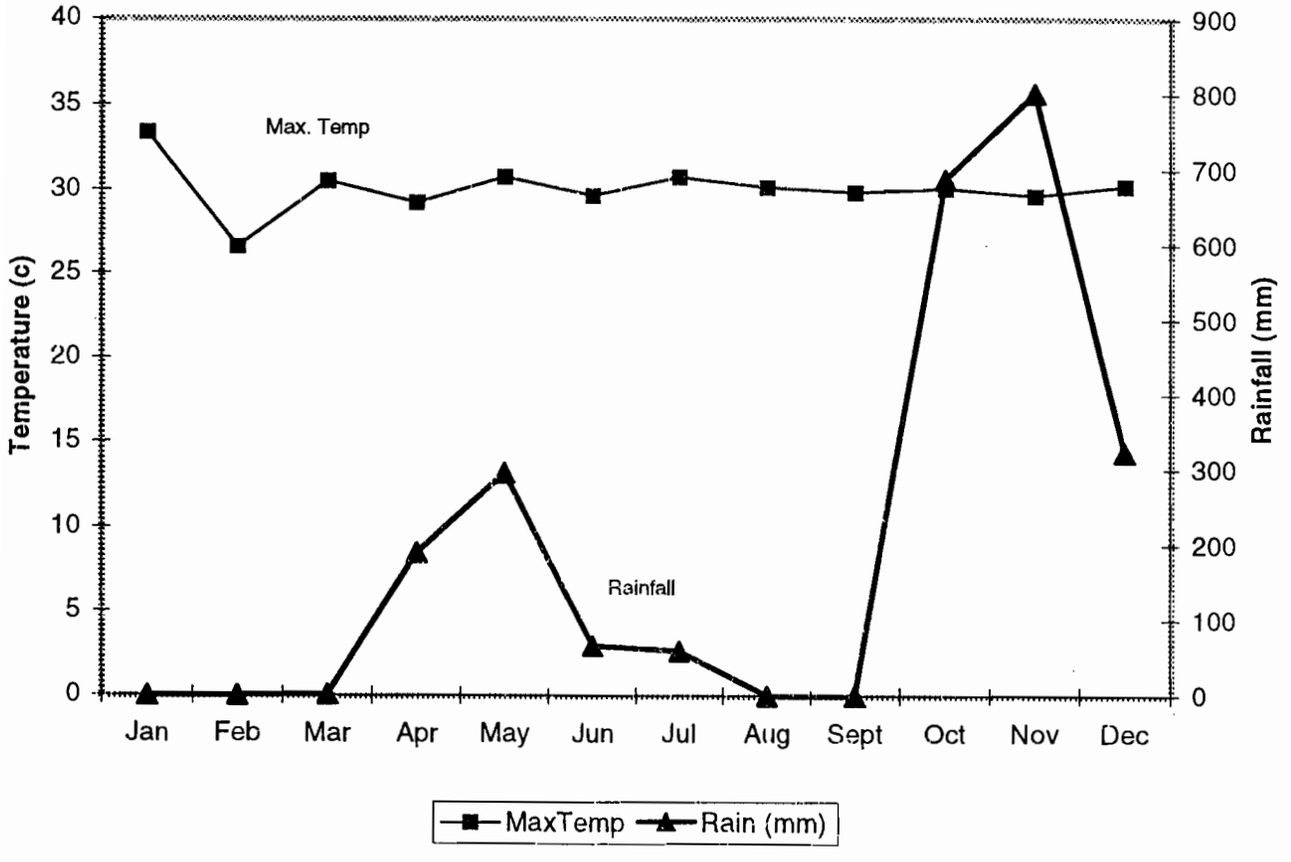

Fig. 2: The abnormal 1997 El-Nino related rainfall and temperature patterns recorded at Mariakani agricultural research station to the north of study area. The two rainy seasons are discernible. In normal years the short rains in November are usually much lower, ie of the order 100mm/month.

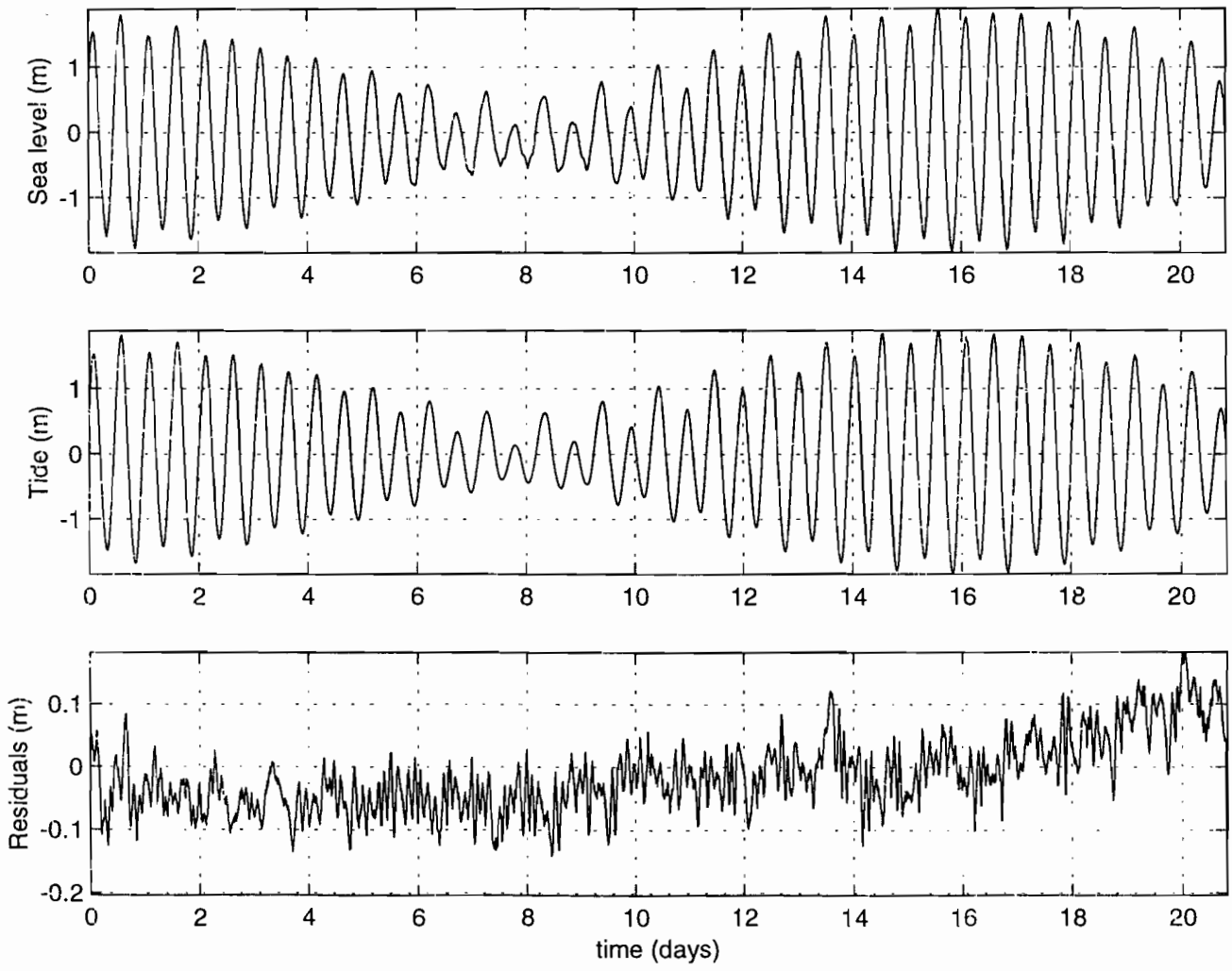

Fig. 3: (a) The observed sea level, (b) computed tide and (c) residuals at Stn 6. These are based on measurements conducted in the period between February 2-23, 1999. The low amplitude of the residual imply that circulation is mainly driven by the tides.

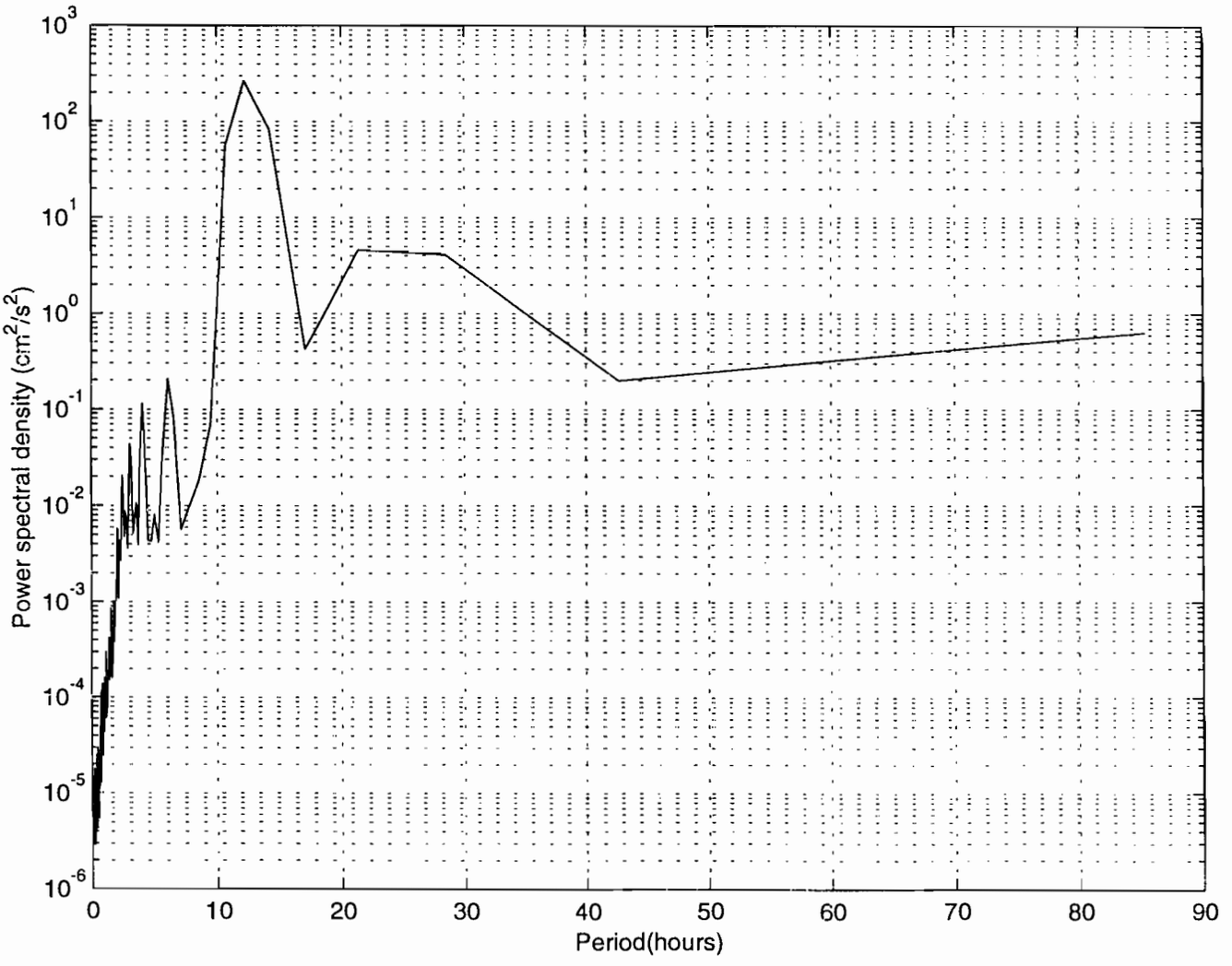

Fig. 4: The spectral energy density analysis of the sea level data measured in the period February 2-23, 1999. The dominant peak low frequency variation is associated with tidal forcing.

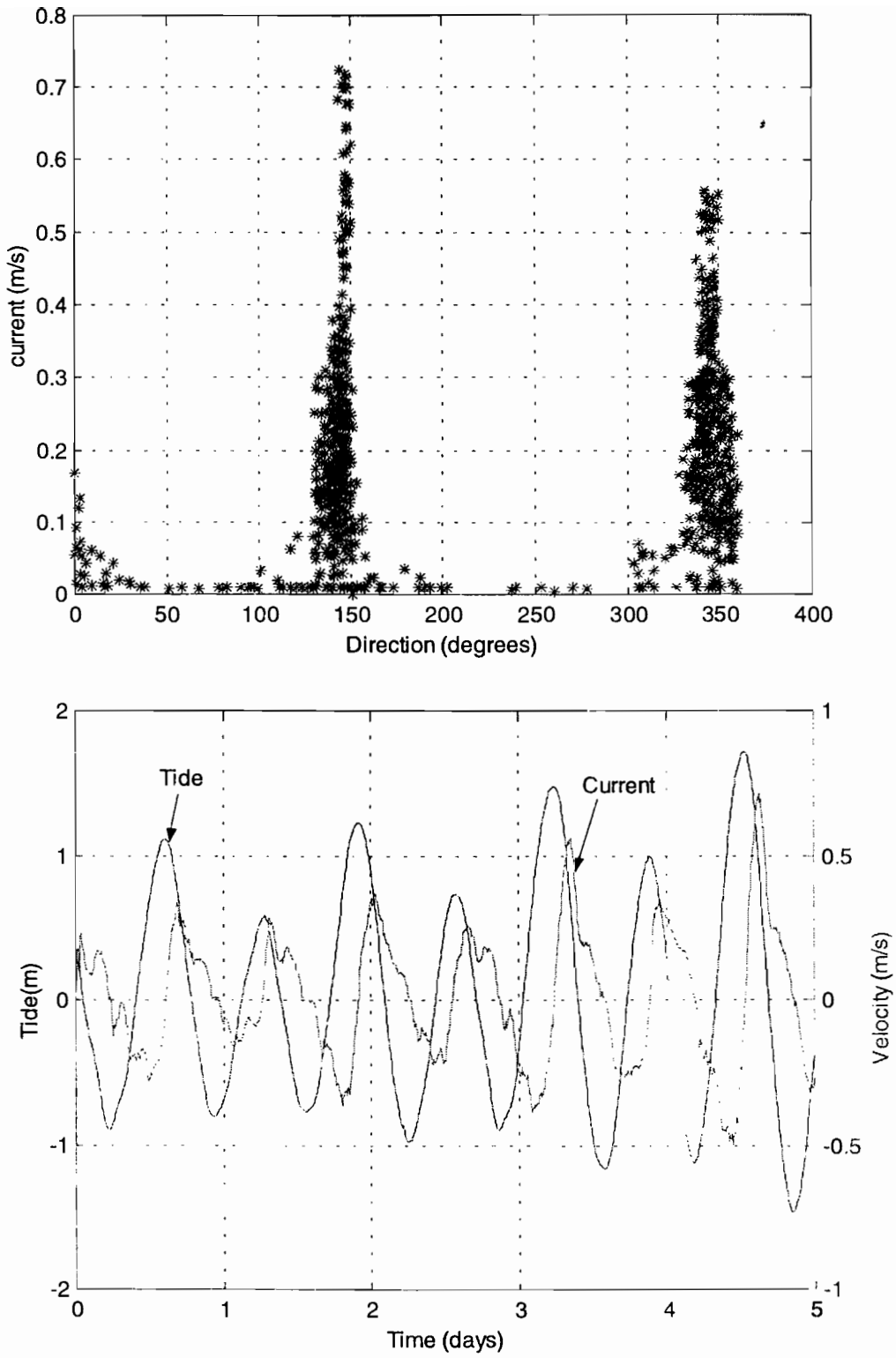

Fig. 5: (a) Current direction and magnitude and, (b) the relationship between current velocity and sea level at Stn 6 in the period between January 26-30, 1998. The starting time is 1225 h.

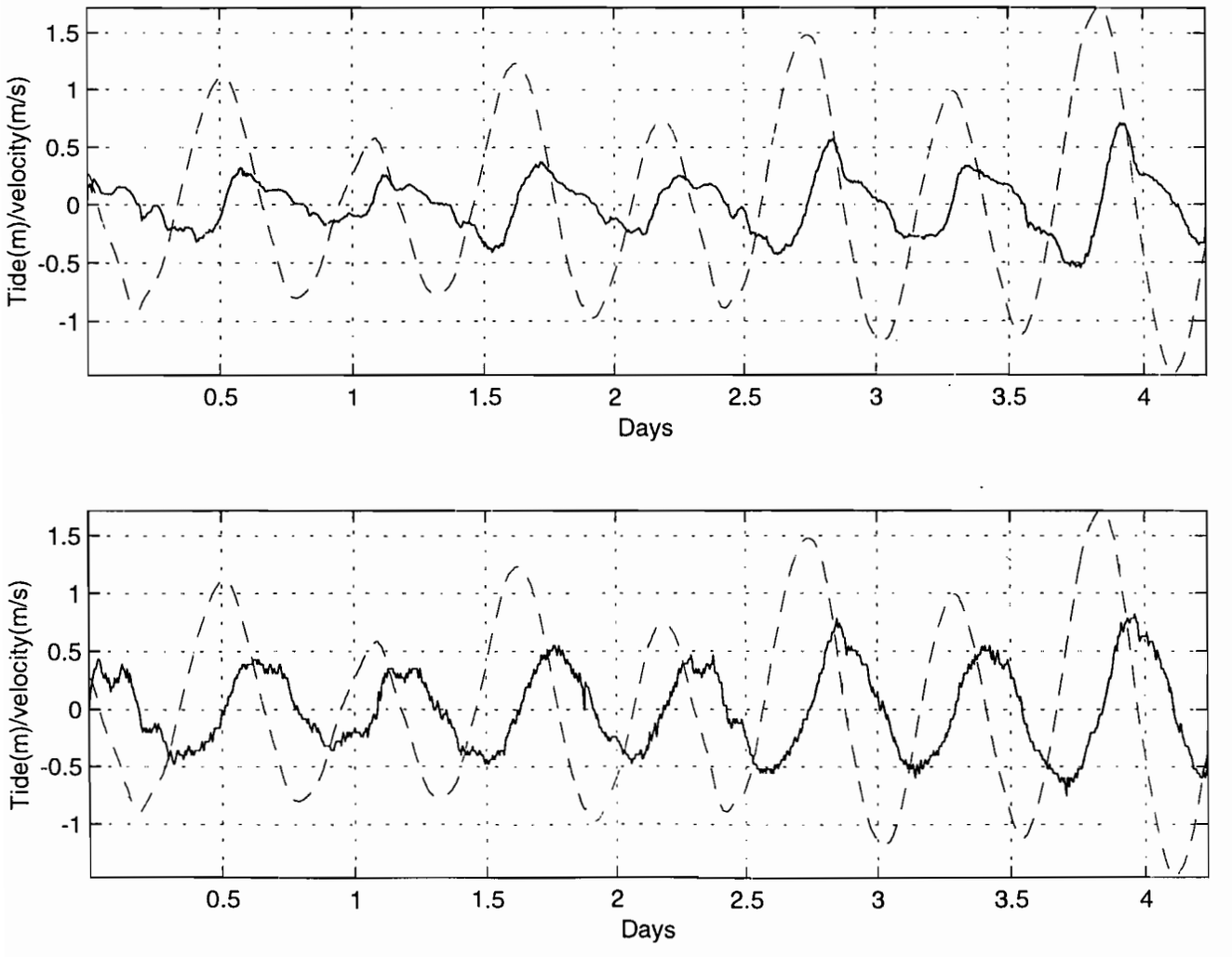

Fig. 6: (a) The measured current velocities (__) with sea level (_ _) and, (b) computed current velocities (__) with sea level (_ _) at Stn 6 in the period between January 26-30, 1999, starting at 1225 hours.

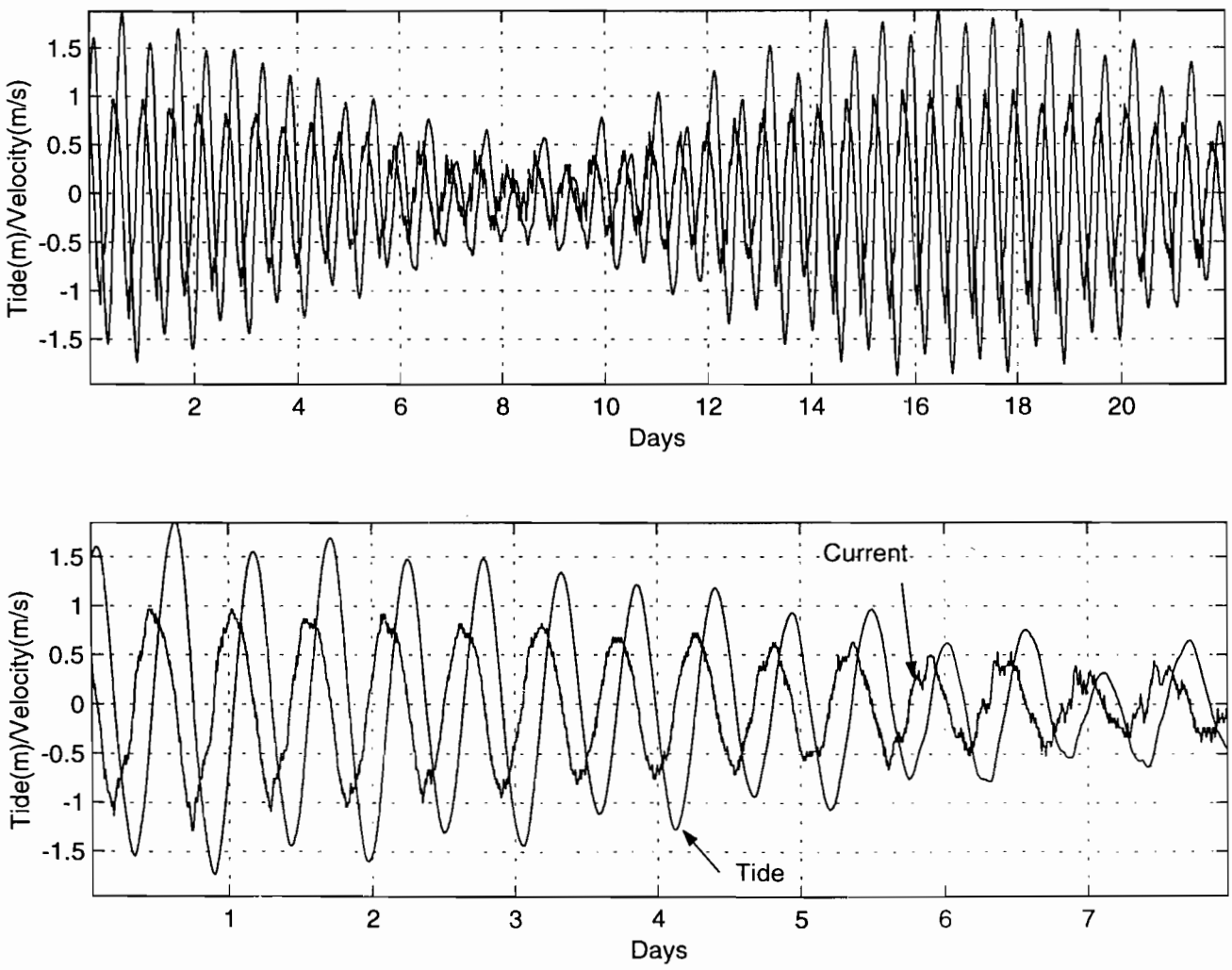

Fig. 7: (a) The relationship between computed current velocity and tide at Stn 6 for the period between February 2-23, 1999 and, (b) for selected period between February 15-23, 1999 starting at 1600 hours.

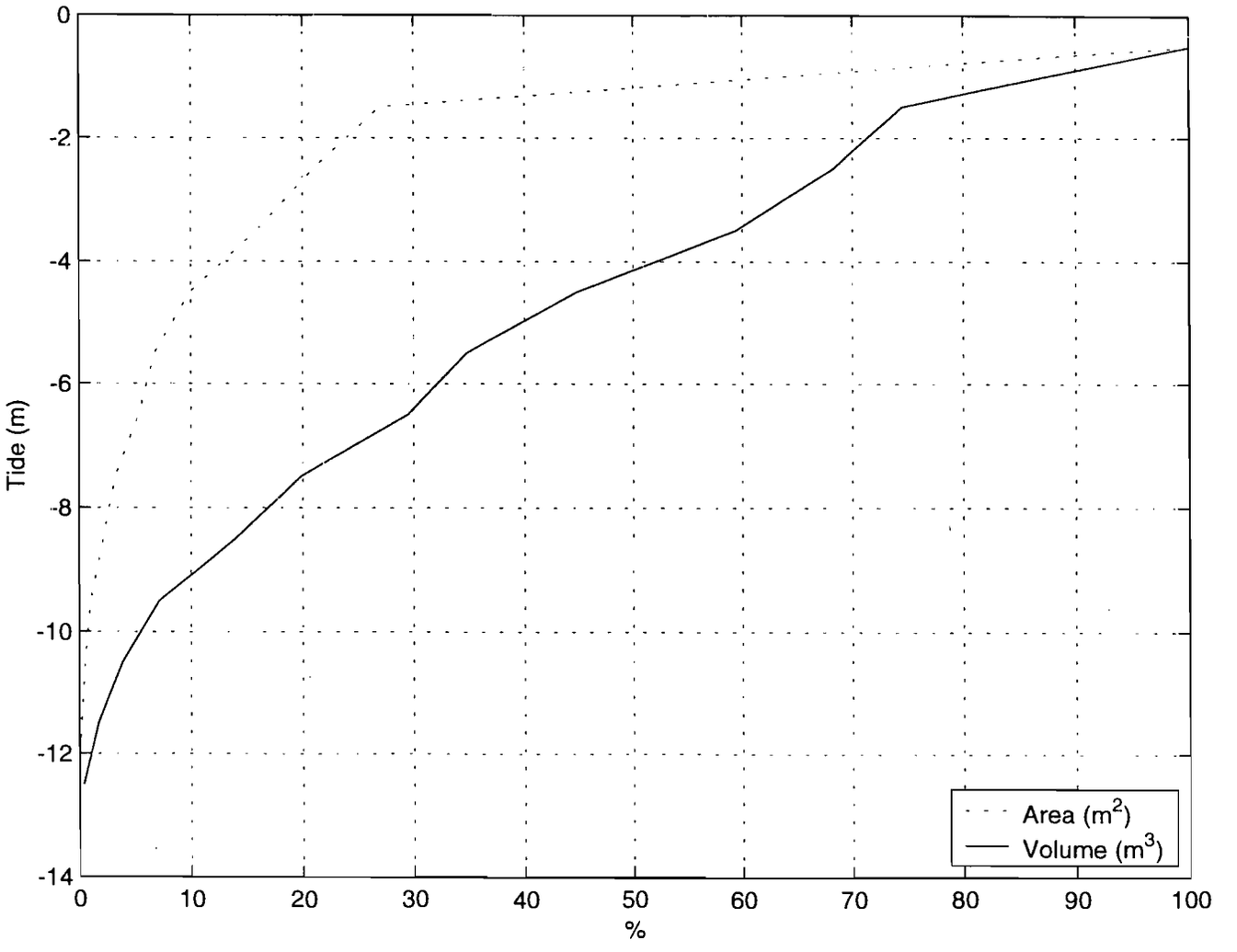

Fig. 8: The hypsometric curve of Port-Reitz mangrove wetland above Stn 7. Reference level approximates yearly maximum sea level. Mean sea level (MSL) is at about –2.3m.

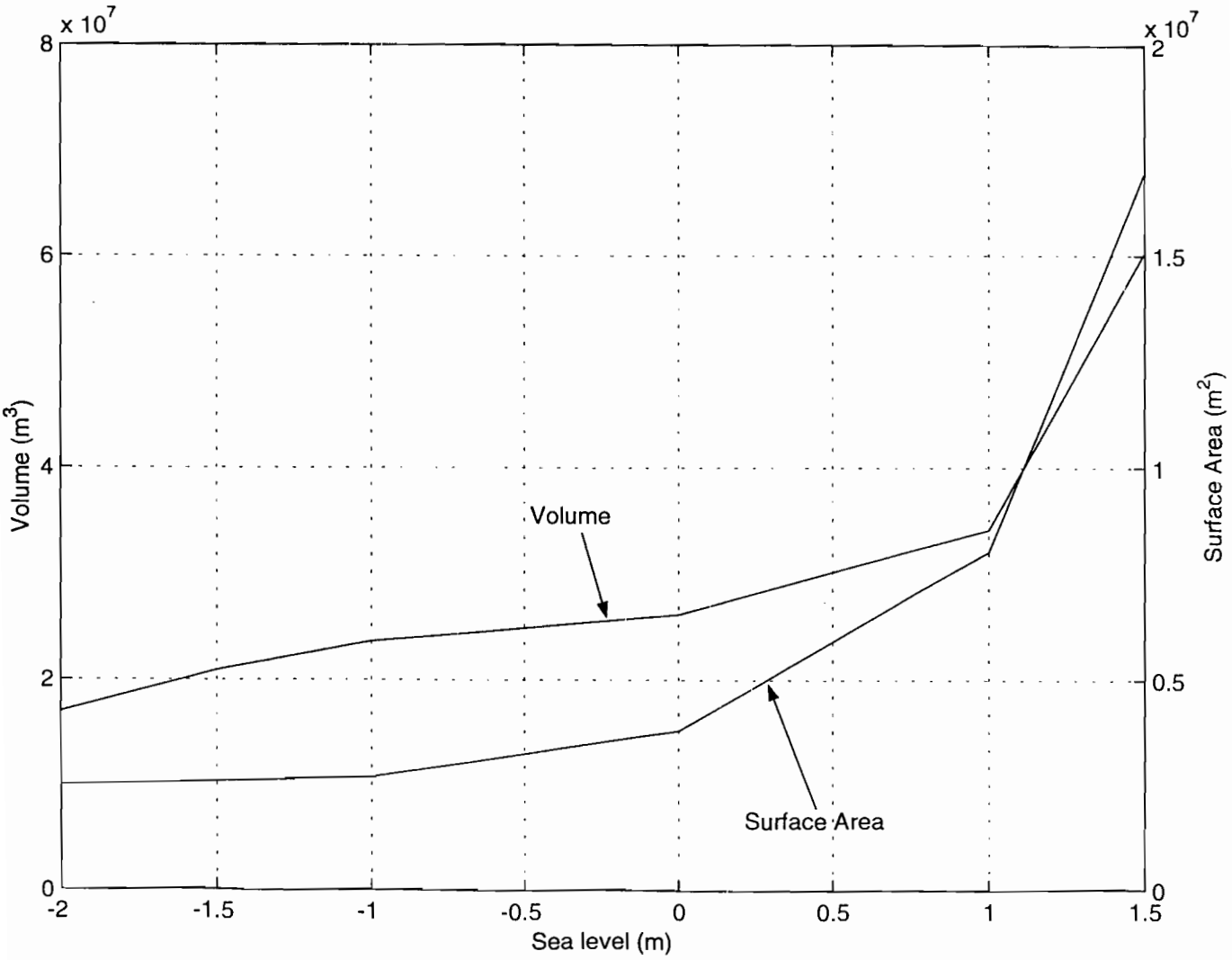

Fig. 9: Surface area and volume as a function of sea level above Stn 7. Due to influx of flood tide water into the shallow mangrove zone, the mean water depth at high tide (sea level: +1.5m) is lower than that at low waters (sea level: -1.5m) when water is restricted in the deep tidal channel. MSL at 0.

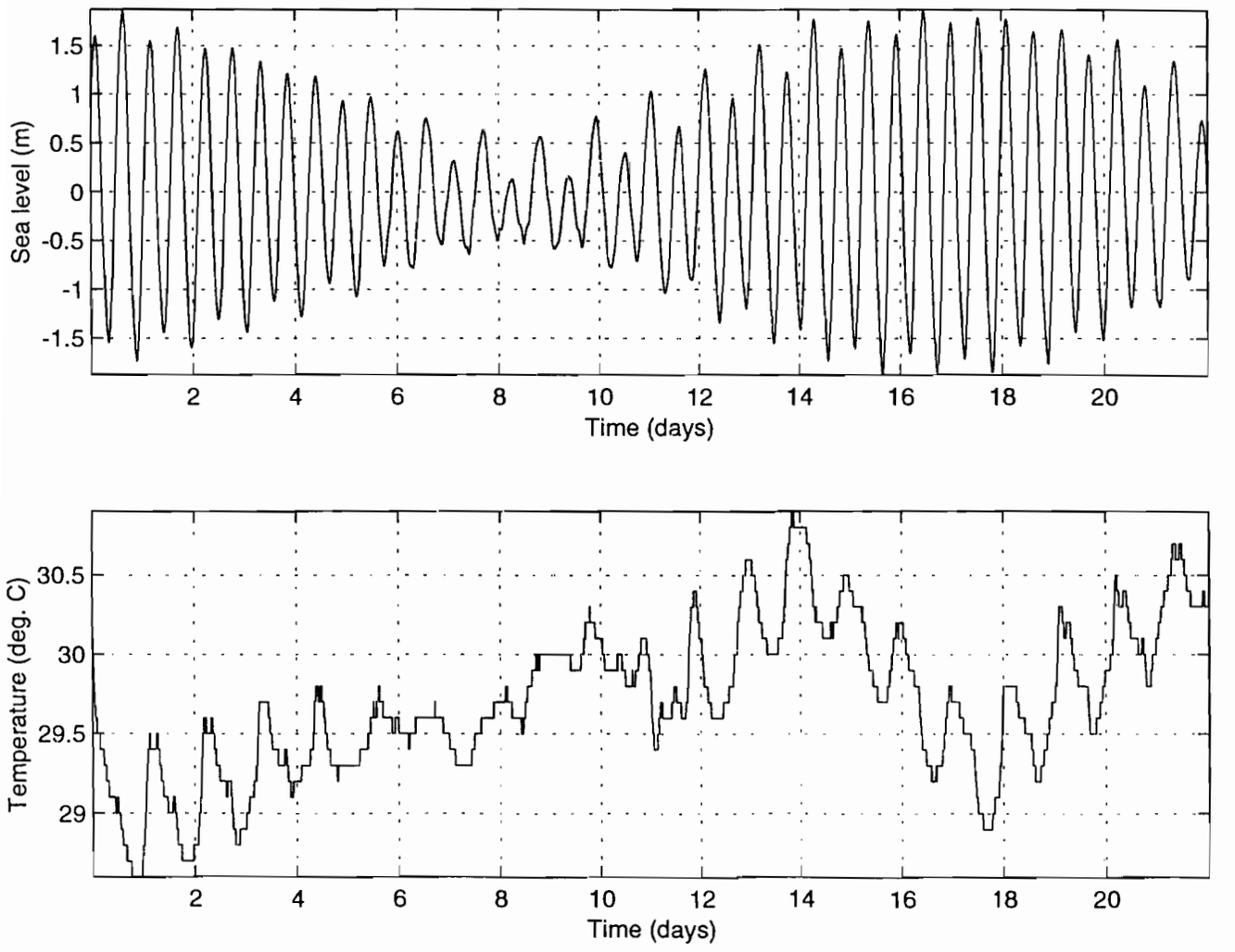

Fig. 10: The patterns of temperature variations based on time-series measurements at Stn 6.

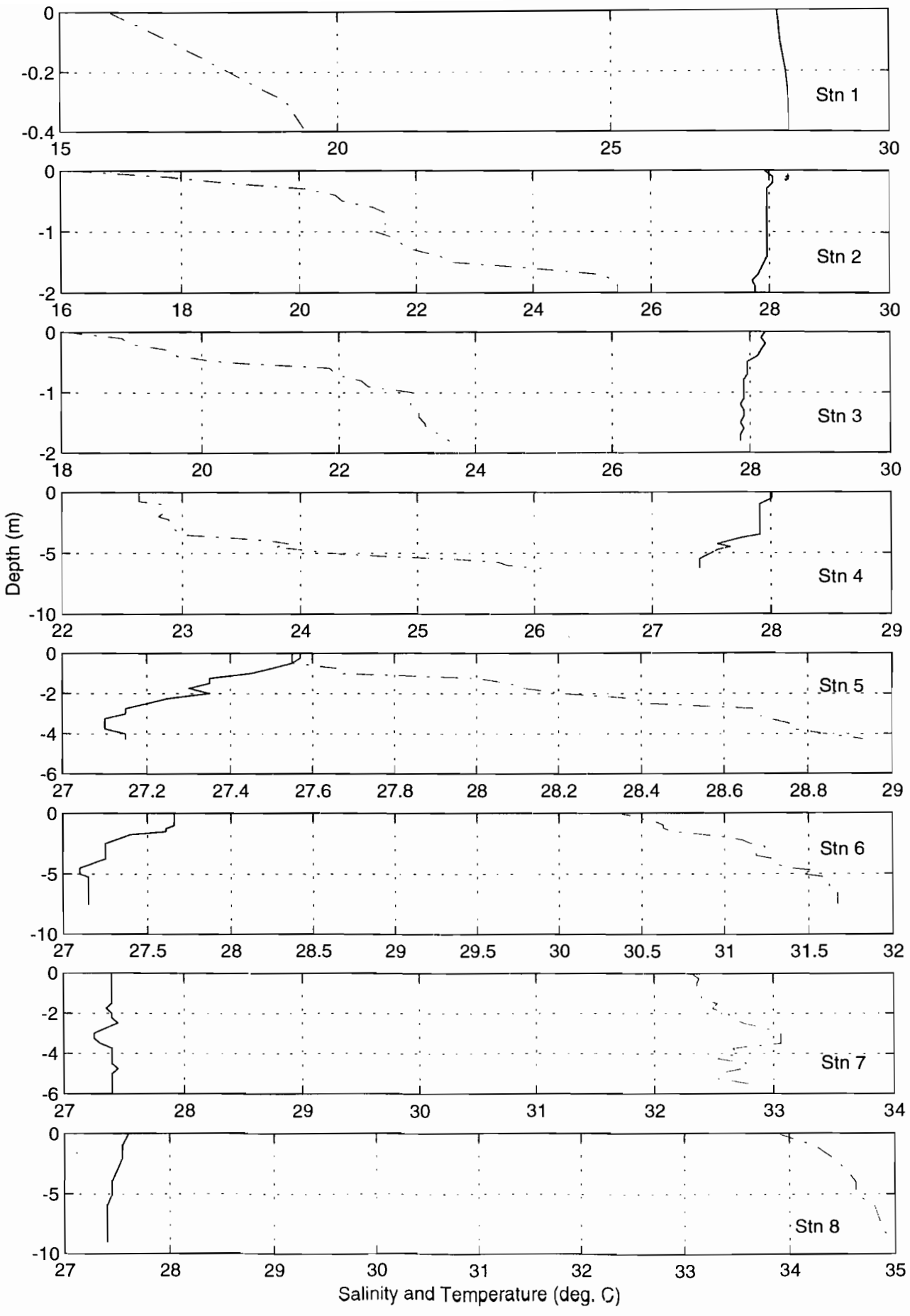

Fig. 11: The vertical temperature (___) and salinity (_._.) profiles in different stations as on 11 June 1998 at the end of the long-rain season.

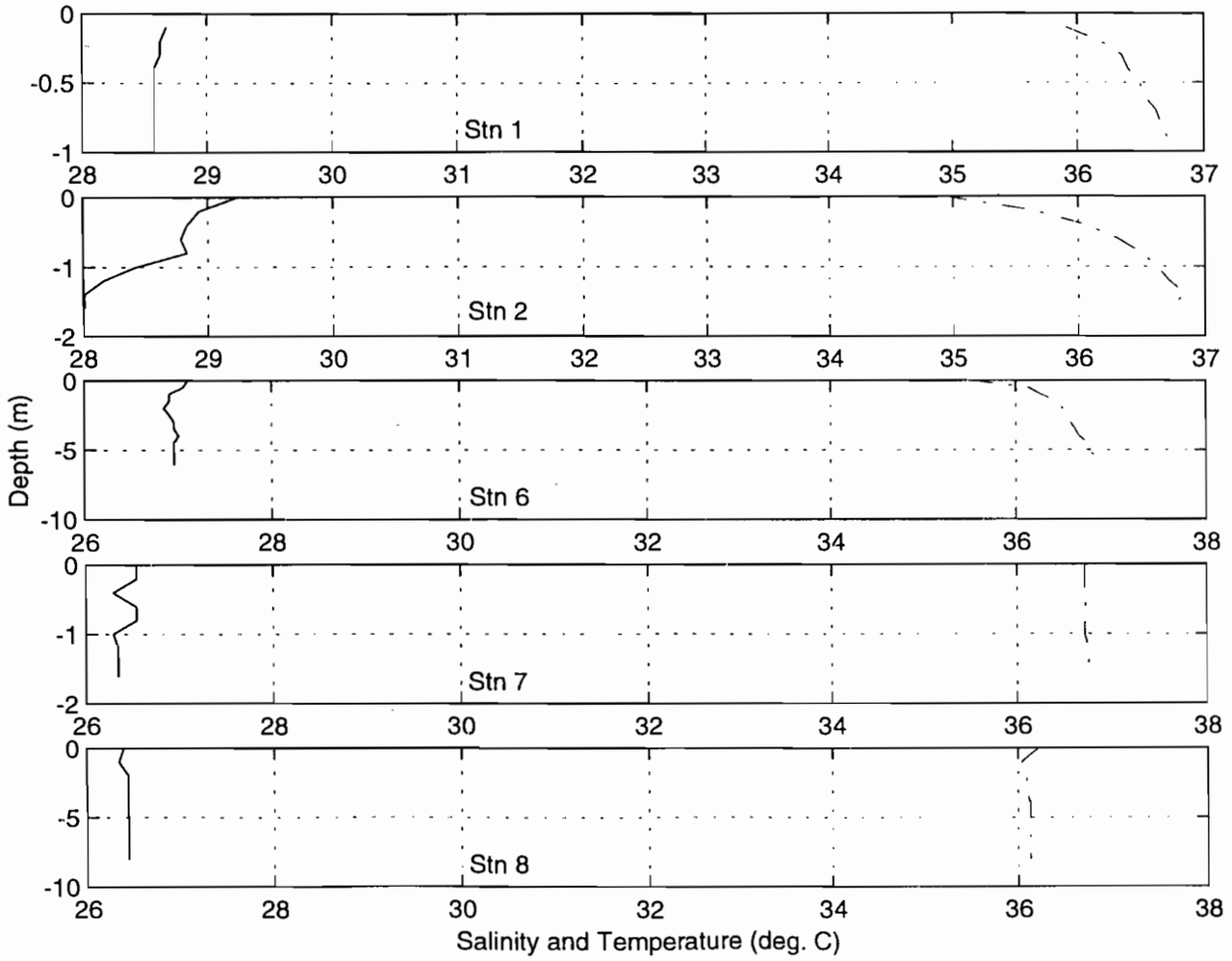

Fig. 12: The vertical temperature (___) and salinity (_._.) profiles in different stations as on 8 October 1998 during dry season.

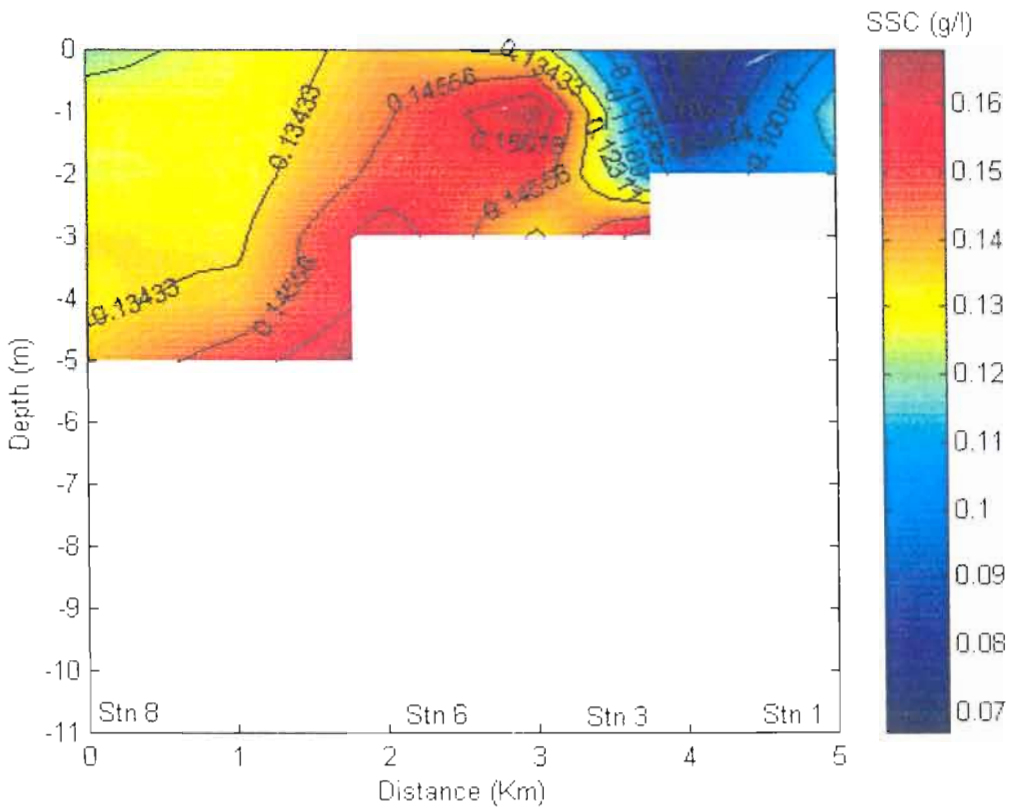

Fig. 13: A contour plot showing SSC distribution in the creek 2 hours after spring low waters. The plot is based on measurements conducted on September 22, 1998 with Orbital backscatter sensor coupled to the MicroTide pressure gauge.

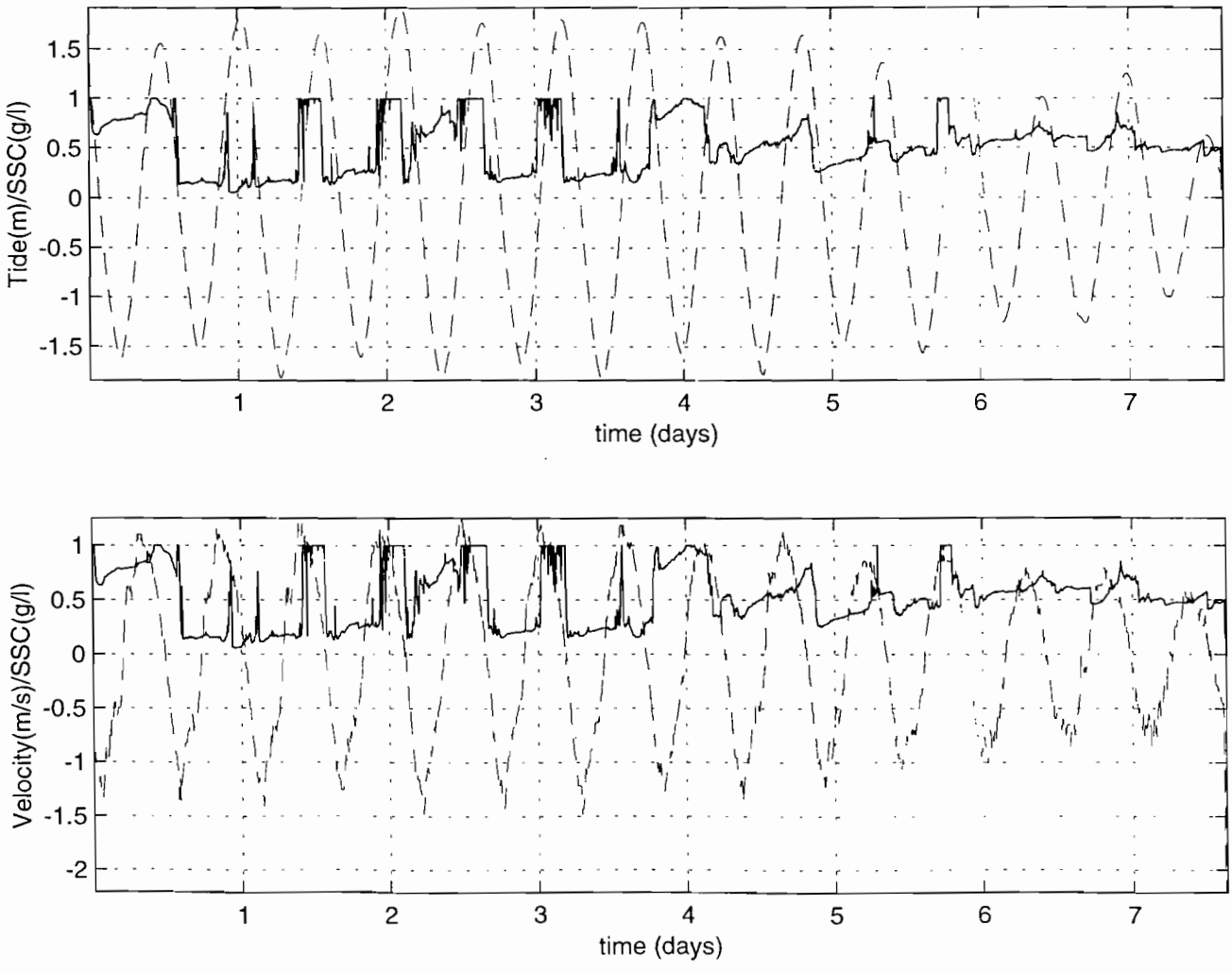

Fig. 14: (a) The relationship between SSC (___) and tide (_ _) and, (b) SSC (___) and current velocities (_ _) at Stn 6 in the period between February 15-23,1999 starting at 1600 h.

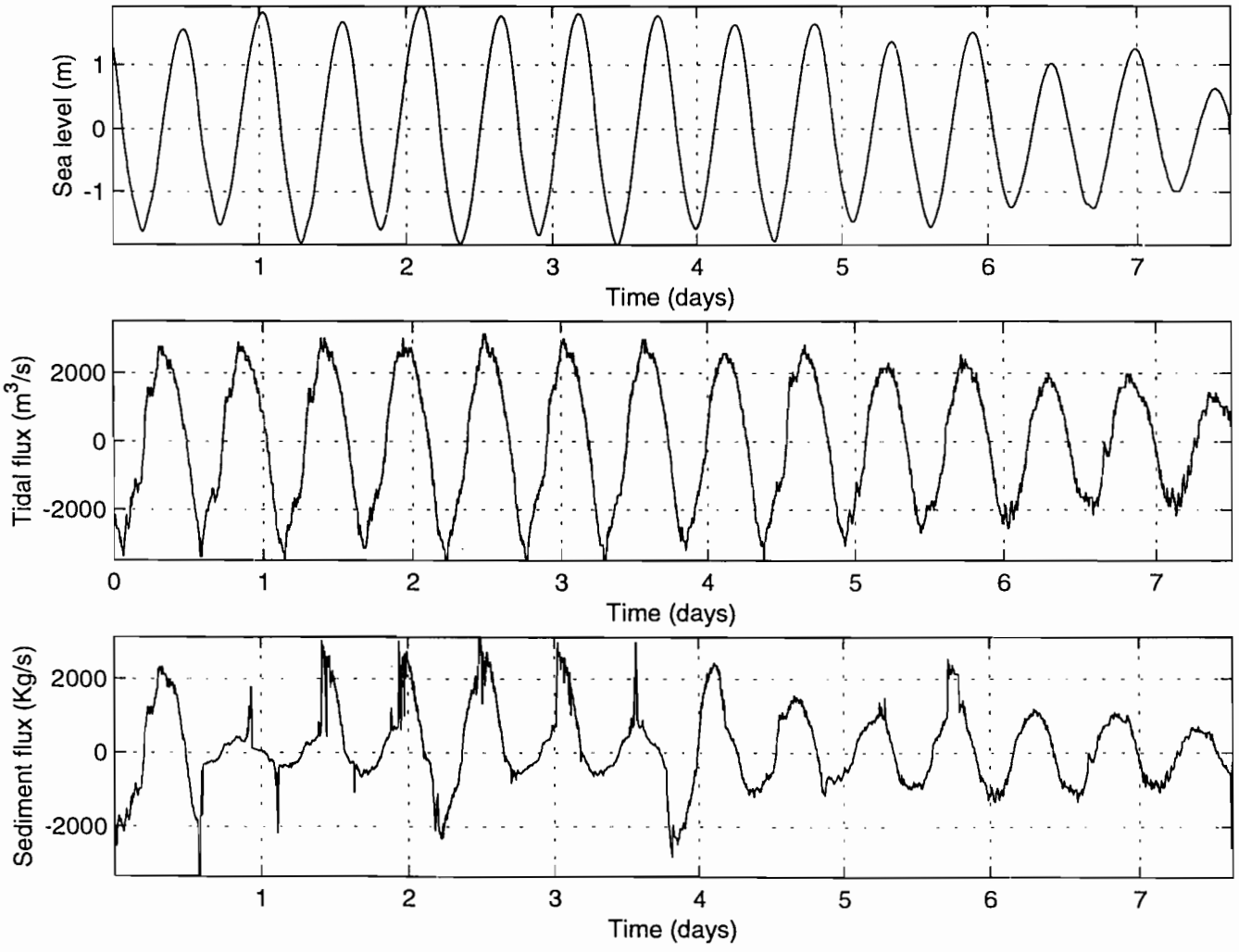

Fig. 15: (a) Sea level, (b) tidal volume and (c) suspended sediment fluxes at Stn 6 during February 15-23, 1999 starting at 1600h.

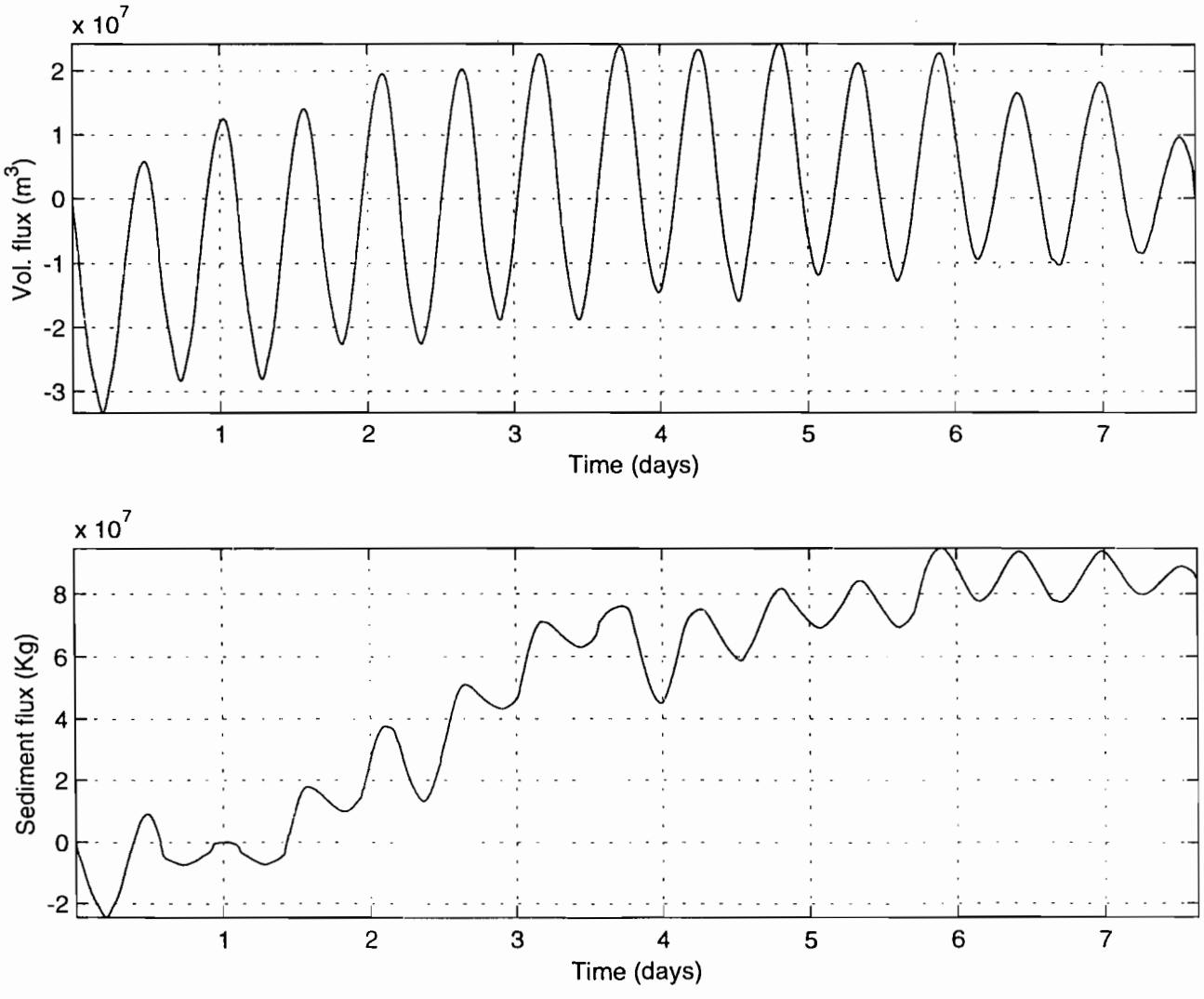

Fig 16: (a) Integrated volume and (b) suspended sediment mass flux in the Mwache creek based on Feb-15-23, 1999 sea level and SSC measurements at Stn 6.

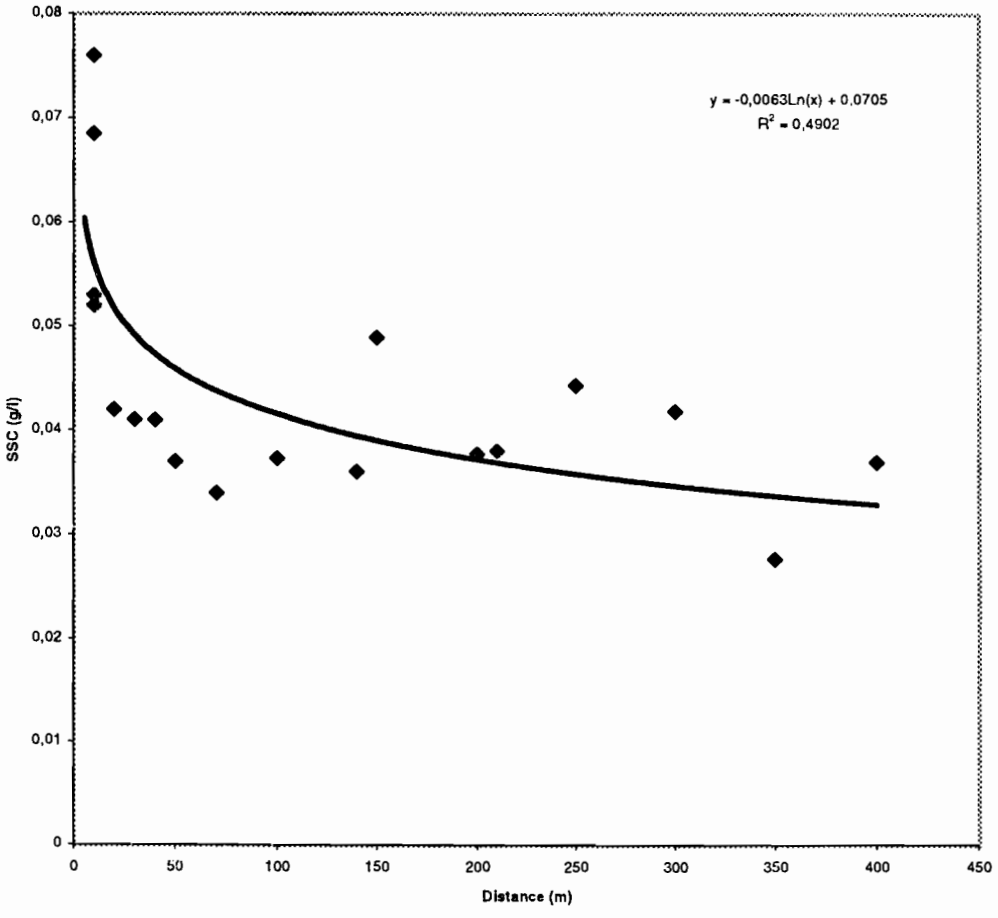

Fig. 17: (a) The spatial variation of SSC across Mwache mangrove forest.

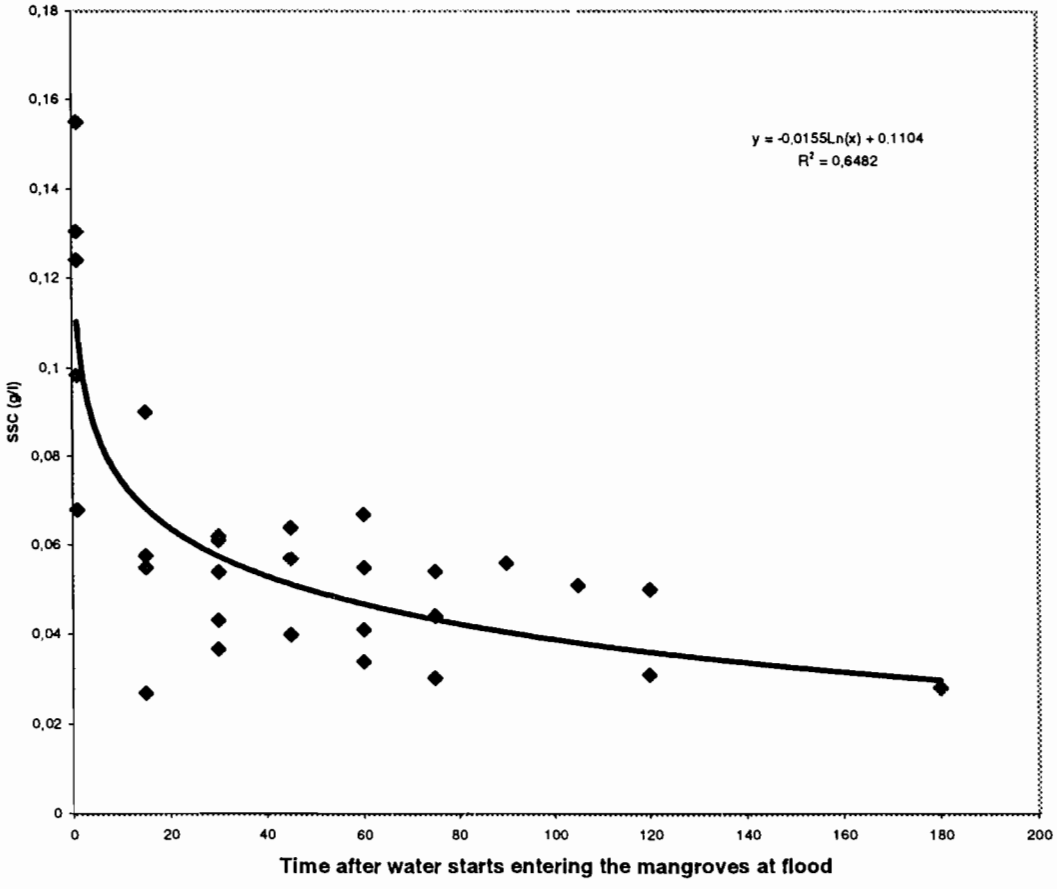

Fig. 17: (b) The temporary variation of SSC in the middle of the transect located inside the Mwache mangrove forest swamp.

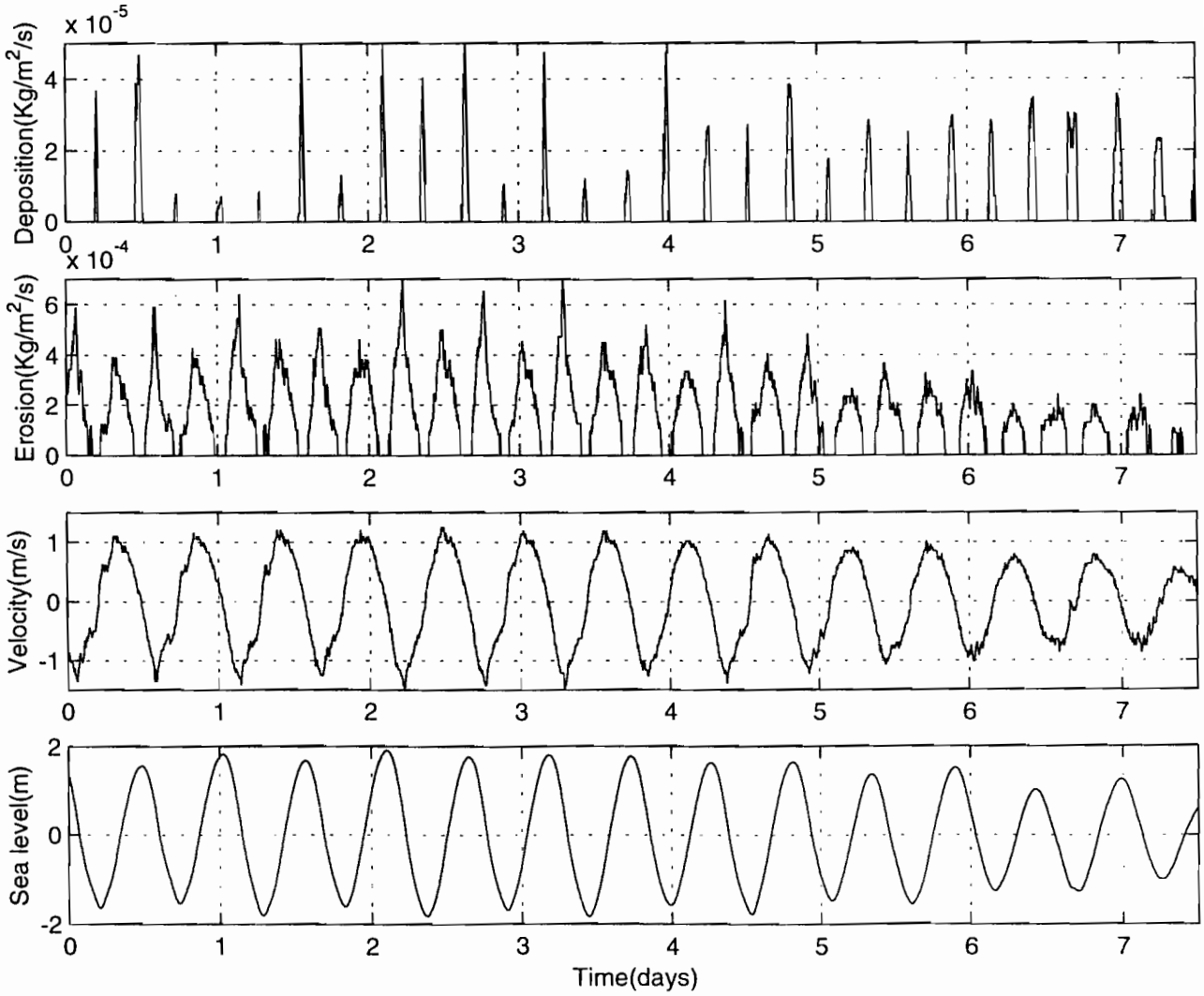

Fig. 18: (a) Sediment deposition, (b) erosion, (c) corresponding tide and (d) tidal currents at Stn 6 in the period between Feb. 15-23, 1999.

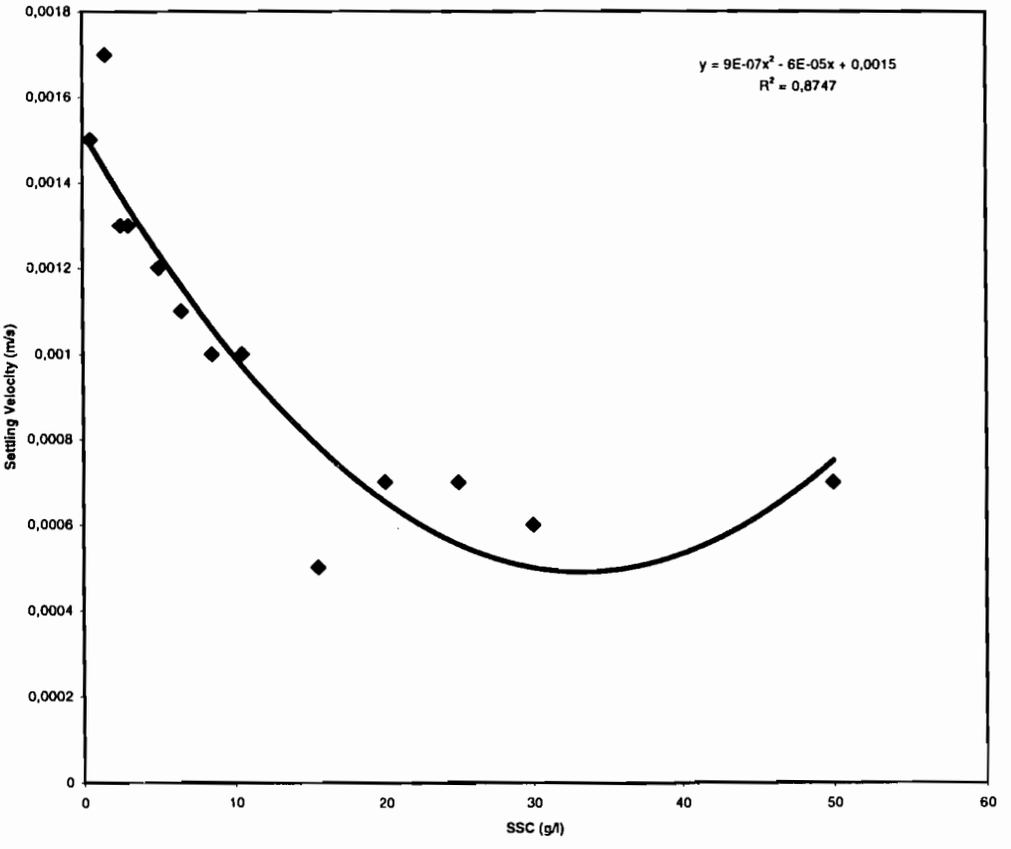

Fig. 19: The relationship between SSC and sediment particle settling velocity using channel bed sediment samples taken at Stn 6 during low waters.

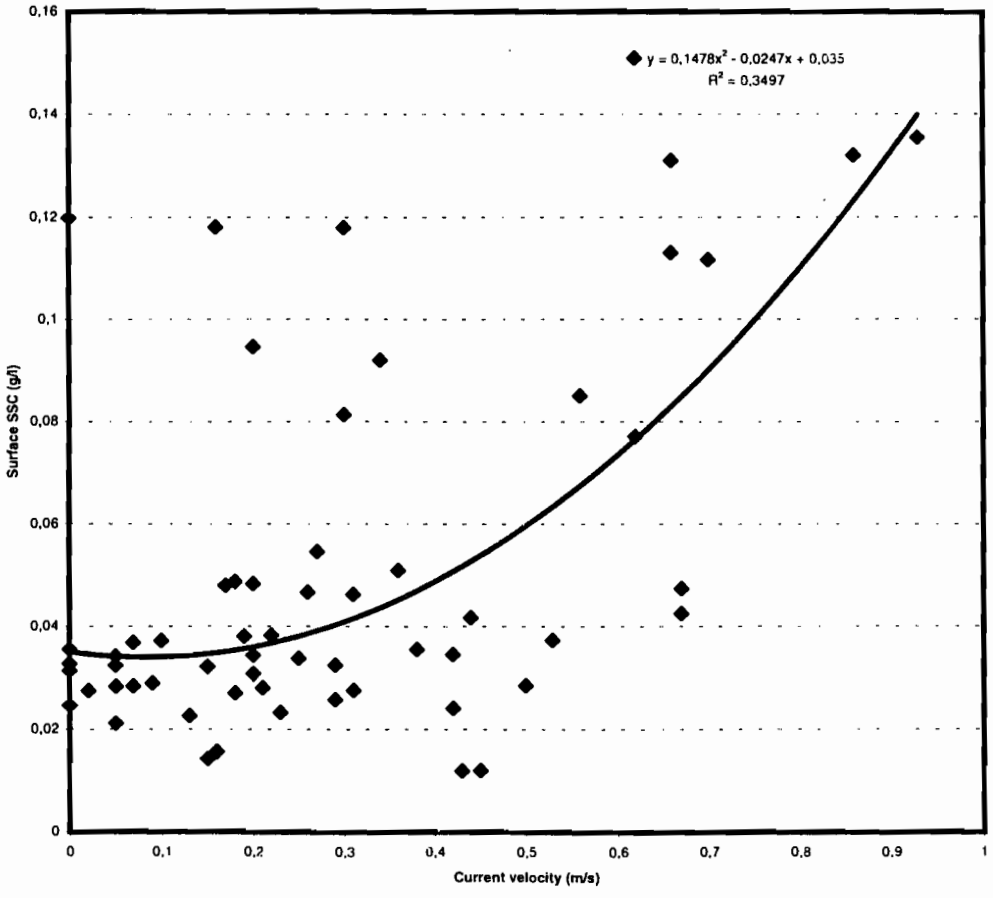

Fig. 20: The scatter plot showing the relationship between current velocities and near surface (0.1-0.2m from water surface) SSC at Stn 6 based on measurements conducted in the period between June and November 1999.

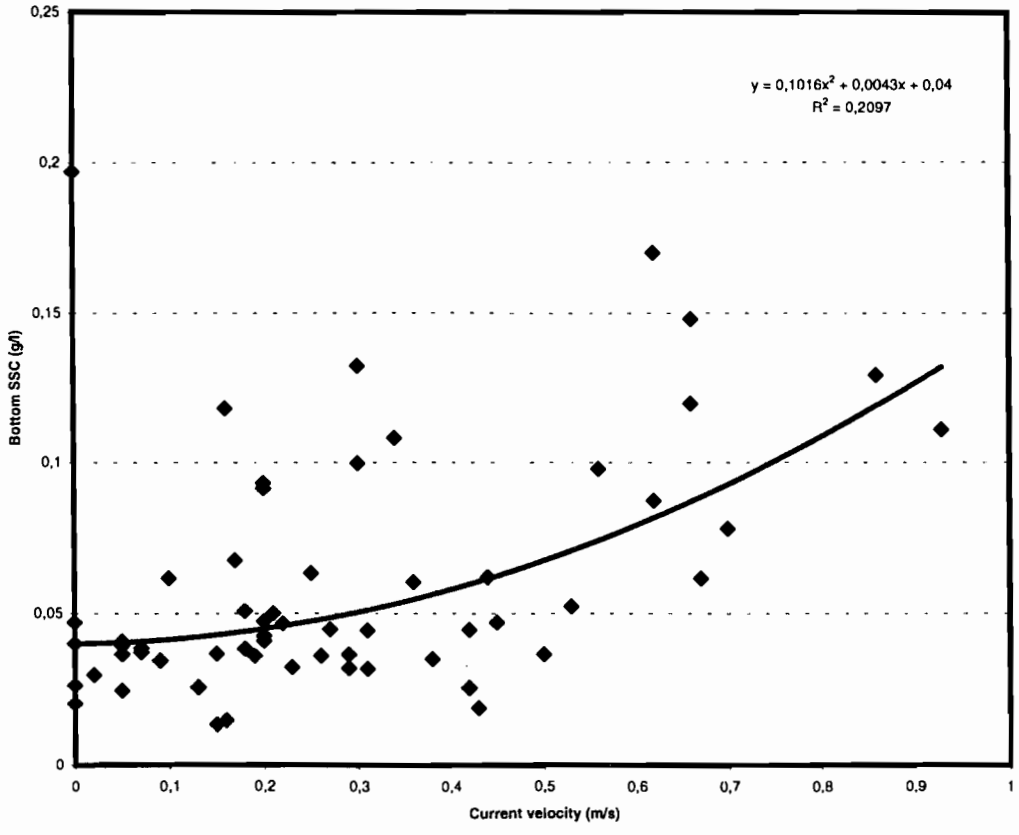

Fig. 21: The scatter plot showing the relationship between current velocities and near bottom (0.1-0.3m from bed) SSC at Stn 6 based on measurements conducted in the period between June and November 1999.

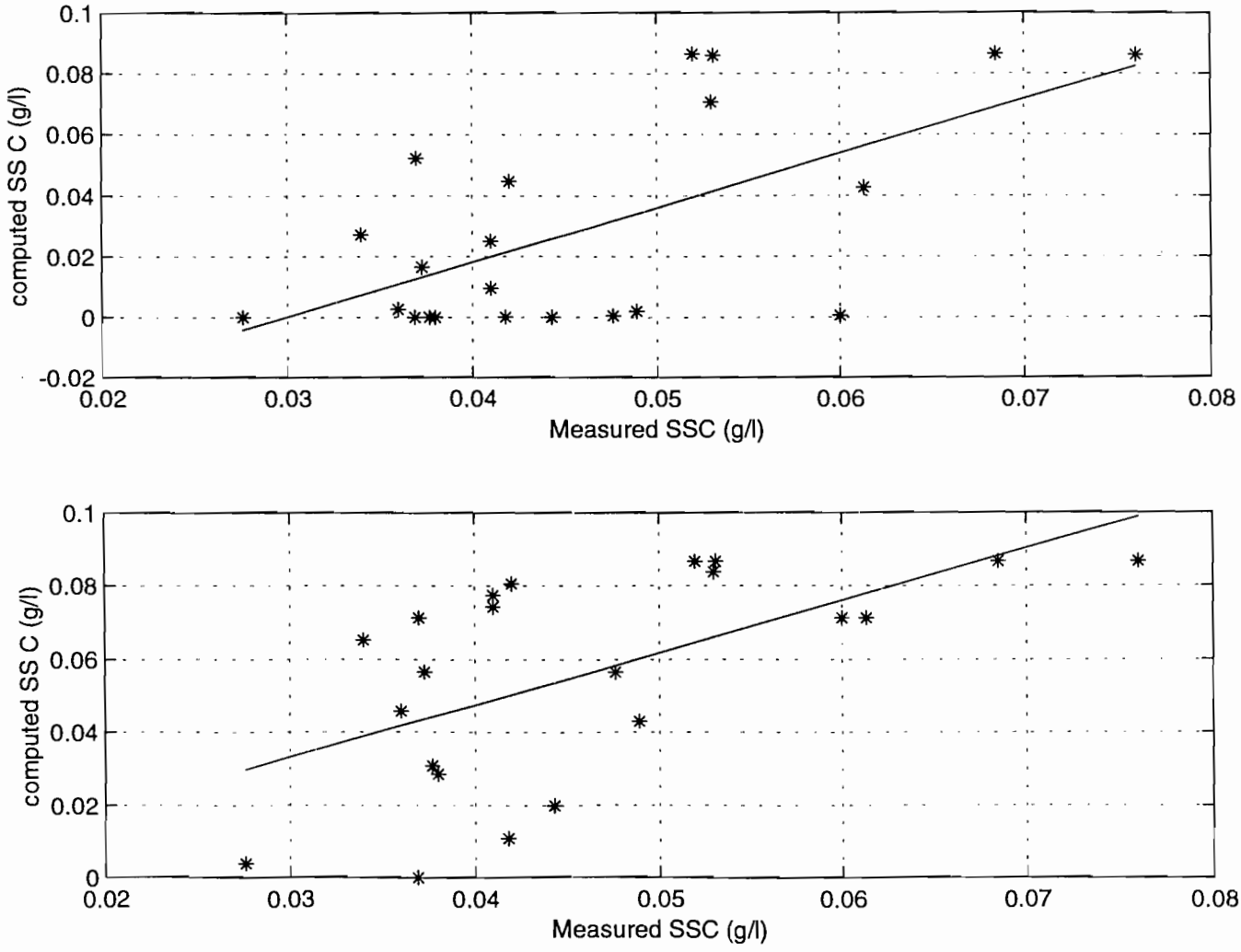

Fig. 22: The comparison between the measured and computed SSC using (a) Furukawa-Wolanski equation and (b) an alternative one proposed in this study.